Accepted Manuscript

Design, synthesis and biological evaluation of quinoline derivatives as HDAC class I inhibitors

Chen Chen, Xuben Hou, Guohua Wang, Wenyan Pan, Xinying Yang, Yingkai Zhang, Hao Fang

PII: S0223-5234(17)30231-3

DOI: 10.1016/j.ejmech.2017.03.064

Reference: EJMECH 9324

To appear in: *European Journal of Medicinal Chemistry*

Received Date: 1 February 2017

Revised Date: 23 March 2017

Accepted Date: 25 March 2017

Please cite this article as: C. Chen, X. Hou, G. Wang, W. Pan, X. Yang, Y. Zhang, H. Fang, Design, synthesis and biological evaluation of quinoline derivatives as HDAC class I inhibitors, *European Journal of Medicinal Chemistry* (2017), doi: 10.1016/j.ejmech.2017.03.064.

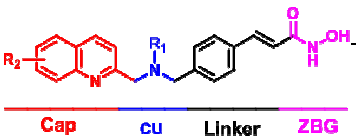

Cpd.	R_1	R_2	IC_{50}		
			HDAC1 (nM)	HDAC8 (nM)	K562 (μM)
4a	H	6-H	72.5±0.5	442±72	0.51±0.01
4e	H	6-Cl	95±1.0	911±32	0.36±0.02
Vorinostat			106±0.0	7469±560	1.95±0.26

Design, synthesis and biological evaluation of quinoline derivatives as HDAC class I inhibitors

Chen Chen [a], Xuben Hou [a,b], Guohua Wang [a], Wenyan Pan [a], Xinying Yang [a], Yingkai Zhang [b], Hao Fang [a*]

[a] *Department of Medicinal Chemistry, Key Laboratory of Chemical Biology (Ministry of Education), School of Pharmaceutical Sciences, Shandong University, 44, West Culture Road, 250012, Jinan, Shandong, PR China*

[b] *Department of Chemistry, New York University, New York, New York 10003 United States*

***Address correspondence to this author:**
Prof. Hao Fang, Department of Medicinal Chemistry, School of Pharmacy, Shandong University, 44 West Culture Road, Jinan, PR China.
E-mail: haofangcn@sdu.edu.cn
Tel. 86-531-88382019
Fax. 86-531-88382548

Abstract:

Inhibition of histone deacetylase(HDAC) has been regarded as a potential therapeutic approach for treatment of multiple diseases including cancer. Based on pharmacophore model of HDAC inhibitors, a series of quinoline-based N-hydroxycinnamamides and N-hydroxybenzamides were designed and synthesized as potent HDAC inhibitors. All target compounds were evaluated for their *in vitro* HDAC inhibitory activities and anti-proliferative activities and the best compound **4a** surpass Vorinostat in both enzymatic inhibitory activity and cellular anti-proliferative activity. In terms of HDAC isoforms selectivity, compounds **4a** exhibited preferable inhibition for class I HDACs, especially for HDAC8, the IC_{50} value (442 nM) was much lower than that of Vorinostat (7468 nM). Subsequently, we performed class I & IIa HDACs whole cell enzyme assay to evaluate inhibitory activity in whole cell context. Compounds **4a** and **4e** displayed much better cellular activity for class I HDACs than that for class IIa HDACs, which indicated that **4a** and **4e** might be potent class I HDAC inhibitors. Meanwhile, flow cytometry analysis showed that compound **4a** and **4e** can promote cell apoptosis *in vitro*.

Keyword:

Quinoline
Hydroxamic acid
Class I HDACs
Anti-proliferative
Class I celluar activity
Pro-apoptosis activity

1. Introduction

At present, cancer has been a leading cause of death and a major public health problem with increasing incidence and mortality. It has been widely believed that widespread epigenetic dysregulation that interacts extensively with underlying genetic mutations lead to tumorigenesis[1]. Histone deacetylases (HDACs) and histone acetyltransferases (HATs) played a pivotal role in epigenetic regulation of gene expression and had pleiotropic effects at the cellular and systemic levels[2]. HDACs removed the acetyl groups of lysine residues, leading to chromatin structure becoming contraction and therewith repressing transcription. HATs opposed the effect of HDACs, which referred to histone acetylation and relaxed chromatin structure resulting in enhancing transcription [3]. There was a balance for histone acetylation and deacetylation between the activities of both HATs and HDACs in normal cells. Human HDACs had 18 members and they were divided into four classes. Class I HDACs acted a vital part in tumorigenesis through forming complexes with other proteins. For example, HDAC1 connected with retinoblastoma tumor suppressor protein and formed complex, which was a key controlling factor on cell proliferation and differentiation. The transcriptional repressor complex, producing by association of HDAC2 with YY1, a mammalian zinc-finger transcription factor, played an essential role in transcriptional

regulation[4]. HDAC8 has been proved to be important for cancer cell survival, when HDAC8 was knocked down, the growth of certain cancer cell lines (HeLa and HCT116) was suppressed[5]. HDAC8 expression level was also positively correlated to poor prognosis and metastasis of neuroblastoma[6]. Thus, HDAC inhibitors (HDACIs) have capabilities to control acetylation level of histones and non-histone proteins by inhibiting HDAC enzymes, which then produce a variety of effects on cancer cells, such as cancer cell arrest, differentiation and active cell apoptosis [7].

Attributed to decades of synthetic efforts, five HDAC inhibitors (Vorinostat, Romidepsin, Belinostat, Panobinostat and Chidamide) have been applied to the clinical therapy (Fig. 1) [8] and more than twenty candidates have been initiated in clinical trials in monotherapy or combination therapy. Vorinostat, Romidepsin, Belinostat and Panobinostat were approved by US FDA for treatment of cutaneous T-cell lymphoma (CTCL), peripheral T-cell lymphoma (PTCL) and multiple myeloma (MM), respectively[9-12], while Chidamide has been only approved in China[8]. Based on literature investigations, most HDAC inhibitors possessed a three-motif pharmacophore model, comprising of a zinc binding group (ZBG), a linker group and a surface recognition group (cap group) [13]. The ZBGs chelated zinc ion within HDACs active site and were indispensable for HDAC inhibitory activities. The linker group bound into the acetyl-lysine binding channel and connected the ZBG with the cap group, which further enhanced the HDAC-inhibitor interactions.

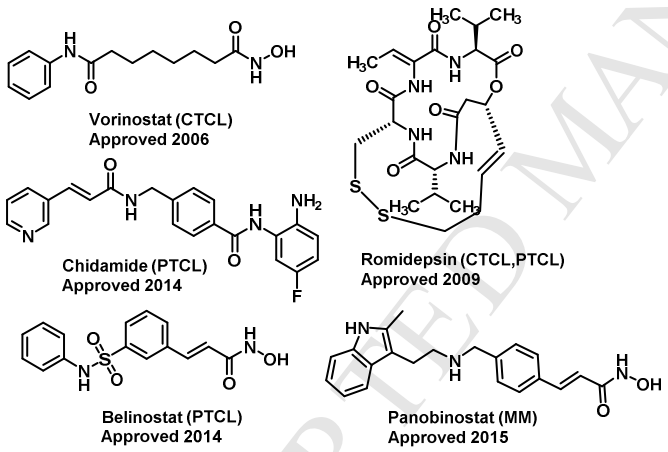

Fig. 1 Approved HDAC inhibitors.

Lots of HDAC inhibitors have been developed by utilizing different heterocycles as the cap group, such as thiadiazole[14, 15], saccharin[16], purine[17, 18]，N-phenylquinazolin[19] and quinoline[20]. Importantly, quinoline hydroxamic acid derivatives has been proved to exert HDAC inhibitory activities and anti-proliferative activities in our previous study [20]. Meanwhile, N-hydroxycinnamamide and N-hydroxybenzamide, which serve as both ZBGs and linker groups, were widely used fragments in current HDACIs design[21, 22]. Three HDACIs (pracinostat, belinostat and panobinostat) with N-hydroxycinnamamide fragment have been approved by FDA and several N-hydroxybenzamide HDACIs are in clinical trials[23]. Guided by these structural analyses above, we developed a series of new HDACIs by utilizing quinoline derivatives as cap group and utilized N-hydroxycinnamamide and N-hydroxybenzamide as the ZBG and linker groups. This article reports the synthesis and preliminary biological evaluation of these compounds.

2. Results and discussion

2.1. Chemistry

The routes used for synthesis of the entire target compounds are outlined in Schemes 1-3. As shown in Scheme 1, starting materials **1a-1g** and **2a-b** were commercially available or easily synthesized according to literature [20, 24]. Compounds **1a-1g** reacted with **2a-2b** according to reductive amination to obtain **3a-3g**. Compounds **3a-3g** were directly converted to N-hydroxycinnamamides **4a-4g** by treating with hydroxylamine. In order to increase the structural diversity, N-alkylation were performed to introduce R_1 group to get **5a-5g**, which were converted to N-hydroxycinnamamides **6a-6g**. As shown in Scheme 2, **9a-9b** were easily synthesized by Wittig-Horner reaction. Reductive amination of **1a-1g** with substituted aniline yielded **7a-7g**, which next did coupling reaction with **9a** or **9b** to get **10a-10i**. Compounds **10a-10i** were next converted to N-hydroxycinnamamides **11a-11i**. As shown in Scheme 3, final N-hydroxybenzamides **14a-14d** and **16a** were synthesized following the similar procedures as shown in Scheme 1.

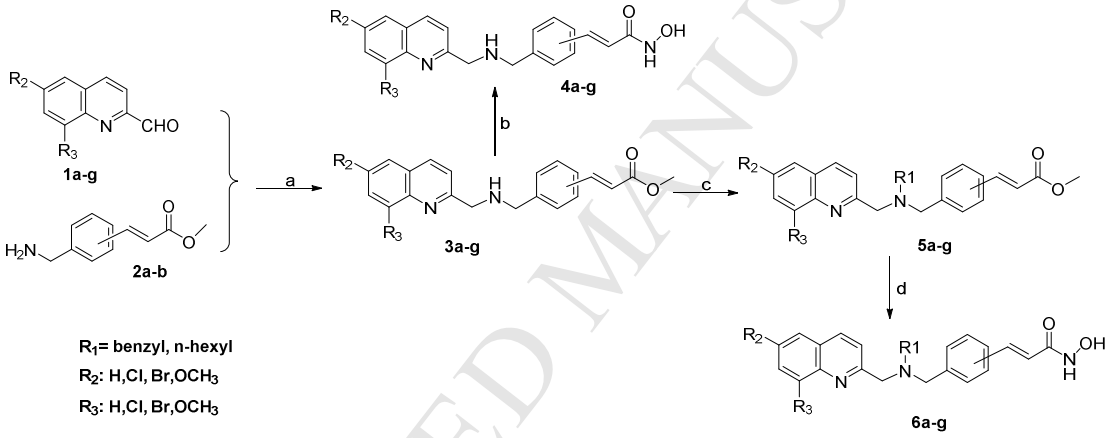

Scheme 1. Synthesis of target compounds **4a-g** and **6a-g**. Reagents and conditions: (a) MeOH, 65°C, 1h; $NaBH_4$, rt, 1h; (b) NH_2OH•HCl, KOH, MeOH, rt, 4 h; (c) R_1-X， DMSO, DIEA, 50°C, 2-4h; (d) NH_2OH•HCl, KOH, MeOH, rt, 4 h.

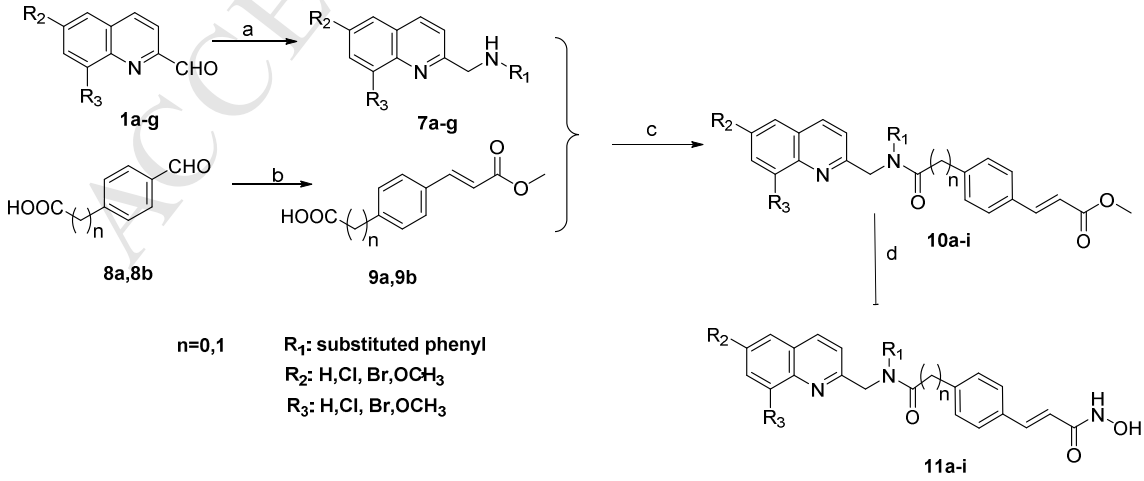

Scheme 2. Synthesis of target compounds **11a-11i**. Reagents and conditions: (a) (i)aniline, formic acid, DCM, rt, overnight; (ii) $NaBH_4$, MeOH, rt, 1h; (b) trimethyl phosphonoacetate, K_2CO_3, H_2O,

rt, overnight; (c) (i) oxalyl chloride, DCM, rt, 1h (ii)$NaHCO_3$, DCM, rt, 4h (d) NH_2OH•HCl, KOH, MeOH, rt, 4 h.

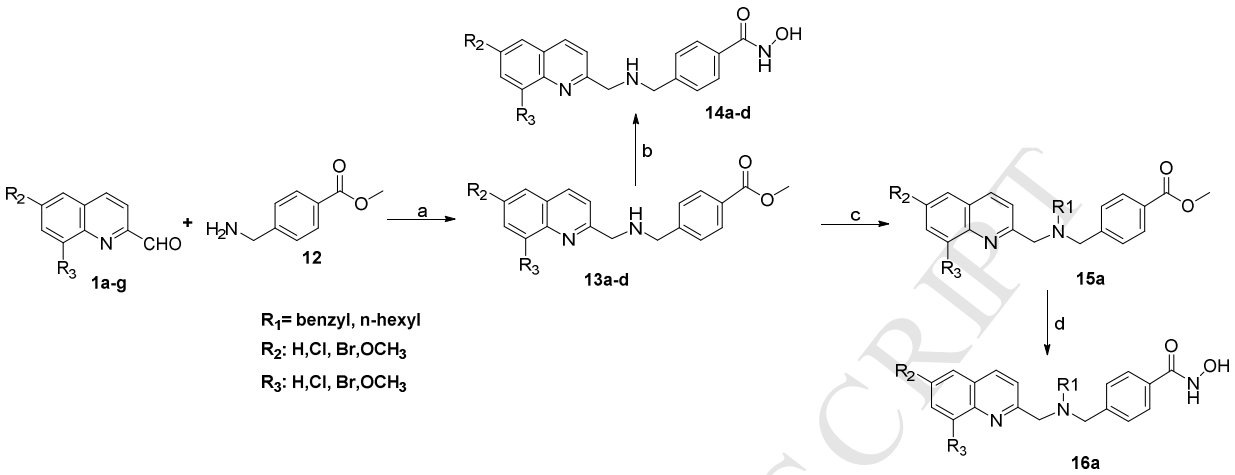

Scheme 3. Synthesis of target compounds **14a-d** and **16a**. Reagents and conditions: (a) MeOH, 65°C, 1h; $NaBH_4$, rt, 1h; (b) NH_2OH•HCl, KOH, MeOH, rt, 4 h; (c) DMSO, DIEA, 50°C, 2-4h; (d) NH_2OH•HCl, KOH, MeOH, rt, 4 h.

2.2. Hela cell extract inhibitory assay

HDAC inhibitory activities of all the target compounds and the positive control drug Vorinostat were evaluated by the Color de Lys™ assay (BMLAK501, Enzo®Life Sciences) including HDAC1&2. Results were summarized as IC_{50} values in Table 1.

As shown in Table 1, the HDAC inhibitory activities of N-hydroxycinnamamides **4a-4f** were superior to N-hydroxybenzamides 1**4a-14d**. As far as N-hydroxycinnamamides were concerned, the HDAC inhibitory activities were influenced by the position of substituents on benzene ring A. For example, compounds with *para*-substituted N-hydroxycinnamamide exhibited better activities than *meta*-substituted N-hydroxycinnamamide derivatives. The differences in linker groups also had significant impacts on inhibitory activities against HDACs. Compounds **11a-11i** with amide groups between quinoline and N-hydroxycinnamamide showed lower activities than compounds **4a-4f** that with amine groups.

Besides, substituents on quinoline ring and amine also had effects on the inhibitory activities against HDACs. Substitution on amine (R_1 groups) decreased the HDAC inhibitory activities. For example, the IC_{50} values of compounds **4a-4g** were lower than that of compounds **6a-6g** (>1000 nM). On the other hand, substituents on quinoline ring (R_2 and R_3 groups) only showed slight effects on potency and the IC_{50} values of compounds **4d**, **4e**, **4f** all distributed between 200-300 nM. Different from our previous study, in which the substituents on the R_2, R_3-position of quinoline enhanced the enzymatic inhibitory activities[20], compound **4a** without any substituent in R_1, R_2, R_3 manifested best enzymatic inhibitory activity with a IC_{50} value of 138 nM against HDAC1&2.

Table 1

The chemical structures and HDACs inhibitory activities of quinoline hydroxamate derivatives.

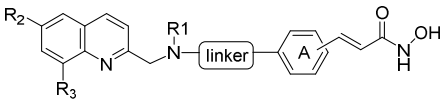

Cpd.	R_1	R_2	R_3	Linker	Substitution of A	IC_{50} (nM)
4a	H	H	H	CH_2	*para*	138±7
4b	H	Cl	H	CH_2	*para*	305±47
4c	H	Br	H	CH_2	*para*	375±55
4d	H	MeO	H	CH_2	*para*	236±76
4e	H	H	Cl	CH_2	*para*	275±64
4f	H	H	MeO	CH_2	*para*	206±51
6a	Bn	H	H	CH_2	*para*	＞1000
6b	Bn	Cl	H	CH_2	*para*	＞1000
6c	Bn	Br	H	CH_2	*para*	＞1000
6d	Bn	MeO	H	CH_2	*para*	＞1000
6e	n-hexyl	Br	H	CH_2	*para*	＞1000
4g	H	Br	H	CH_2	*meta*	559±84
6f	Bn	Br	H	CH_2	*meta*	＞1000
6g	n-hexyl	Br	H	CH_2	*meta*	＞1000
11a	Ph	H	H	C=O	*para*	＞1000
11b	4-Br-Ph	H	H	C=O	*para*	＞1000
11c	4-MeO-Ph	H	H	C=O	*para*	744±48
11d	4-MeO-Ph	H	Cl	C=O	*para*	＞1000
11e	Ph	Br	H	C=O	*para*	＞1000
11f	Ph	H	MeO	C=O	*para*	724±14
11g	Ph	H	H	(C=O) CH_2	*para*	720±97
11h	Ph	Br	H	(C=O) CH_2	*para*	＞1000
11i	Ph	MeO	H	(C=O) CH_2	*para*	560±187

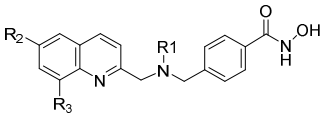

Cpd.	R_1	R_2	R_3	IC_{50} (nM)
14a	H	H	H	＞1000
14b	H	H	Cl	＞1000
14c	H	Br	H	＞1000
14d	H	MeO	H	＞1000
16a	Bn	H	H	836±63
Vorinostat				159±36

2.3 In vitro anti-proliferative assay

Compounds **4a**, **4b**, **4d**, **4e** and **4f** that possessed higher HDAC inhibitory activities than others were selected to evaluate their anti-proliferative activities *in vitro*. MTT assays were performed using five different cancer cell lines including MOLT-4 (acute lymphoblastic leukemia cell), HEL (erythrocyte leukemic cell), PC-3 (prostatic cancer cell), K562 (chronic myelogenous leukemia cell) and Hela (cervical carcinoma cell). The IC_{50} values were summarized in Table 2. Results indicated that all tested compounds showed better anti-proliferative activities in different cancer cell lines compared with Vorinostat. Specially, compound **4e** exhibited the highest anti-proliferative activities in all five cancer cell lines.

Table 2 Anti-proliferative activity of compounds **4a**, **4b**, **4d**, **4e** and **4f**

Cpd.	IC_{50}[a] (μM)				
	MOLT-4	HEL	K562	PC-3	Hela
4a	0.24±0.01	0.15±0.01	0.51±0.01	3.08±0.69	2.20±0.43
4b	0.25±0.02	0.22±0.02	0.72±0.04	4.35±0.35	3.03±0.13
4d	0.23±0.01	0.13±0.01	0.69±0.01	3.70±0.60	2.68±0.08
4e	0.16±0.02	0.11±0.01	0.36±0.02	2.92±0.35	1.82±0.16
4f	0.19±0.02	0.22±0.04	0.75±0.03	4.60±0.50	3.33±0.61
Vorinostat	0.56±0.04	0.25±0.02	1.95±0.26	13.91±0.73	3.55±0.15

[a] IC_{50} were expressed as the mean ± standard deviation of two or three separate determinations

2.4 HDAC isoforms inhibitory activity of representative compounds

To explore the HDAC isoforms inhibitory profile, we chose compounds **4a** with most potent HDACs inhibitory activity and **4e** with highest anti-proliferative activity to perform enzyme inhibitory assays against class I HDACs (HDAC1 and HDAC8) and class II HDAC (HDAC6). Results in Table 3 indicated that compound **4a** and **4e** possessed better inhibitory activities against class I HDACs (HDAC1 and HDAC8) than Vorinostat. For HDAC1, compounds **4a** and **4e** exhibited approximate inhibitory activity with their IC_{50} values slight lower than Vorinostat. For HDAC8, compounds **4a** and **4e** exposed notably inhibitory activity, particularly IC_{50} value of **4a** reached to the 500nM range while IC_{50} value of Vorinostat remained approximately 8μM.

Table 3 HDAC isoforms inhibitory activity of compounds **4a** and **4e**

Cpd.	IC_{50}[a] (nM)		
	HDAC1	HDAC6	HDAC8
4a	72.5±0.5	49.5±2.5	442.0±72.0
4e	95.0±1.0	36.5±5.5	911.0±32.0
Vorinostat	106.0±0.0	14.5±2.5	7468.5±559.5

[a] IC_{50} were expressed as the mean ± standard deviation of two or three separate determinations

2.5 HDAC class I and class IIa whole cell assay

Subsequently, compounds **4a** and **4e** were chosen to perform HDAC whole cell enzyme assay to examine their inhibitory activities as well as and isoforms selectivity in whole cell context. Firstly, HDAC class I cellular assay was conducted in K562 cell line in order to contrast with extracellular inhibitory activity which utilized Hela extract as the enzyme source (mainly contained class I HDACs: HDAC1 and HDAC2). As shown in Table 4, cellular class I HDAC

activity of compound **4a** only had a slightly enhancement compared with extracellular activity (IC_{50} = 138 nM). But compound **4e** displayed substantial increase in cellular class I HDAC activity (IC_{50} = 64 nM) in contrast to extracellular activity (IC_{50} = 275 nM). These results indicated that compounds **4a** and **4e** possess good cell permeability in K562 cell line and their cellular enzyme inhibitory activities were consisted with their anti-proliferative activities.

Furthermore, the result of class IIa cellular assay indicated that class IIa HDACs were less sensitive to compounds **4a** and **4e** as their IC_{50} value ranging in the micromolar concentration. These results in celluar level as well as the HDAC isoforms selectivity results (Table 3) suggested that compounds **4a** and **4e** might be potent class I HDAC inhibitors.

Table 4 HDAC class I and class IIa whole cell assay

Cpd.	HDACs class I cellular IC_{50} (nM) [a,b]	HDACs class IIa cellular IC_{50} (nM) [a,c]
4a	108±13	5213±563
4e	64±8	4208±469
Vorinostat	473±47	42275±2729

[a] Assays were performed in K562 cells; Values are average of at least two determinations, the SD values are < 20% of the mean;

[b] Substrate: Boc-Lys (acetyl)-AMC;

[c] Substrate: Boc-Lys-(ε-trifluormethylacetyl)-AMC.

2.6 Apoptotic assay

It has been previously reported that HDACIs can promote cell apoptosis *in vitro*[25, 26]. Hence, we chose **4a**, **4e** and Vorinostat (positive control) to perform flow cytometry analysis in K562 cells and explore their abilities in inducing cancer cells apoptosis. Results in Fig.2 showed that compounds **4a**, **4e** and Vorinostat could induce apoptosis in a dose-dependent manner. Moreover, compound **4a** and **4e** exerted better pro-apoptosis activities than Vorinostat.

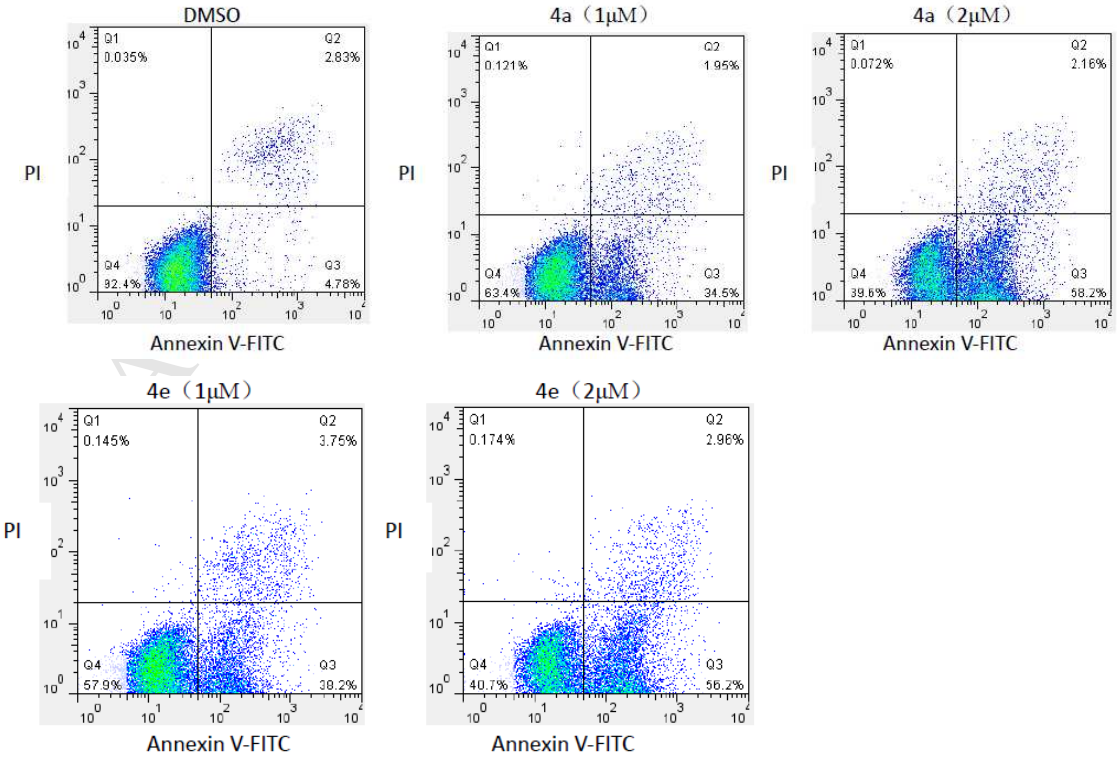

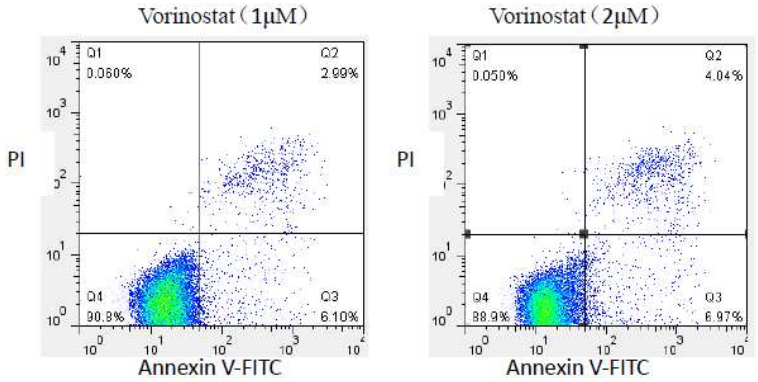

Fig. 2 Inducing apoptosis of K562 cells by **4a**, **4e** and Vorinostat at 1μM and 2 μM after 24 h.

2.7 Molecular docking and molecular dynamics simulation

In order to explore the HDAC-inhibitor binding interactions, we further performed molecular docking as well as molecular dynamics (MD) simulation. Although the biological functions of 11 zinc-dependent HDACs are not fully understood, HDAC1 has been widely recognized as an important cancer relevant target[27]. Thus, HDAC1 and the most potent HDAC1 inhibitor, compound **4a**, were used in our computational study.

Firstly, compound **4a** was docked into the active site of HDAC1 using Autodock Vina[28]. Then, the top-scored conformation was subjected to MD simulation. After energy minimization, heat and equilibration, a 20ns standard MD simulation was performed. As shown in **Fig. 3**, compound **4a** remained in the HDAC1 active site during 20ns MD simulation and became stable after 9ns MD simulation. Clustering analysis was performed using the last 10ns snapshots and representative structure from the biggest cluster suggested the favorable binding mode for compound **4a** with HDAC1. The hydroxamic acid group of compound **4a** chelated with zinc atom properly and formed a series of hydrogen bond interactions with key residues (His140, His141, Asp176, His178 and Tyr301).

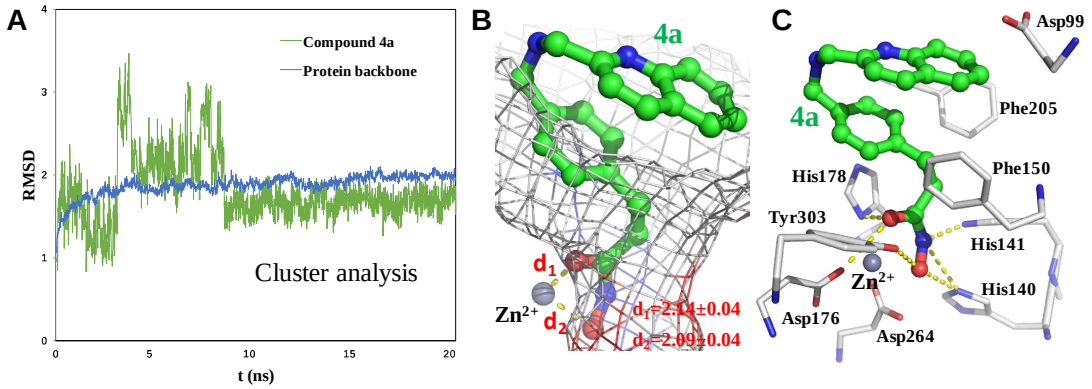

Fig. 3 Predication of the binding mode of compound **4a** in HDAC1. (a) **RMSD** values of compound **4a** (forest green) and HDAC1 protein backbone (blue) during 20ns MD simulation. Snapshots in the last 10ns (grey) were used in clustering analysis. (b) The zinc chelating mode of compound **4a** (green). Average distances were measured using the last 10ns snapshots of MD simulation. Active site of HDAC1 was shown as mesh. (c) Interactions between compound **4a** (green) and HDAC1 residues (white). Hydrogen bonds were shown as yellow dotted line.

3. Conclusions

In our current study, we developed a novel series of quinoline-based N-hydroxycinnamamides and N-hydroxybenzamides, showed their biological evaluation for Hela extract inhibitory activities and anti-proliferative activities on cancer cells. Compound **4a** exhibited higher Hela extract inhibitory activity than Vorinostat. Besides, compounds **4a** and **4e** showed good anti-proliferative activities with IC_{50} being 3-5 folds lower than Vorinostat in K562 and PC-3 cell lines. Meanwhile, HDAC isoforms inhibitory assay and HDAC whole cell assay revealed compounds **4a** and **4e** exhibited selective inhibition against class I HDACs. Moreover, flow-cytometry analysis suggested that compounds **4a** and **4e** induced stronger apoptotic effects in K562 cells than that of Vorinostat, which were in line with their anti-proliferative activities. With the inspiriting results that compound **4a** displayed class I HDACs inhibition and inducing apoptotic effect, it provided a starting point for development of novel HDAC inhibitors targeted to class I HDACs.

4. Experimental section

4.1. Chemistry

Reagents and solvents used were of commercially available LR grade quality and without further purification. All reactions were monitored by TLC on 0.25 mm silica gel plates (60GF-254). UV light, chloride ferric and iodine vapor were used to visualize the spots. Melting points were recorded by the RY-1G electrothermal melting point apparatus without correction. ^{1}H and ^{13}C NMR spectra were recorded on a Brucker DRX spectrometer at 300 MHz or 400 MHz, d in parts per million and J in hertz, using TMS as an internal standard. Significant ^{1}H NMR data are reported in the following order: multiplicity (s, singlet; d, doublet; t, triplet; m, multiplet) number of protons. High-resolution mass spectra (HRMS) were conducted on an Agilent 6510 Quadrupole Time-of-Flight LC/MS deliver. The purity of all targeted compounds was determined to be >95.0% by HPLC. HPLC analysis was performed using an Diamonsil C18 (5μ, 250 mm×4.6 mm) and as a mobile phase gradient from 10% MeCN / 90%H_2O (1‰ formic acid) for 5 min, 10% MeCN / 90%H_2O (1‰ formic acid) to 90% MeCN / 10%H_2O (1‰ formic acid) for 25 min, 90% MeCN / 10%H_2O (1‰ formic acid) for 10 min, a flow rate of 1.0 mL/min.

4.1.1. Methyl (*E*)-3-(4-(((quinolin-2-ylmethyl)amino)methyl)phenyl)acrylate (**3a**)

Aldehyde **1a** (0.16g, 1mmol) and compound **2** (0.19g, 1mmol) was dissolved in MeOH (25ml) and heated at 50 °C for 2 h. After cooling to 0 °C, $NaBH_4$ (3 equiv) was added to the reaction mixture, then the solution was stirred for 2 h at RT. The MeOH was evaporated under reduced pressure and EtOAc was added. The EtOAc layer was washed with a saturated solution of $NaHCO_3$ (×3), brine solution (×3) and then dried and reduced to yield an oil (55%). The oil was purified by column chromatography (DCM / MeOH 120:1). ^{1}H NMR (400 MHz, $CDCl_3$) δ 8.12 (d, J = 8.4 Hz, 1H), 8.06 (d, J = 8.5 Hz, 1H), 7.81 (d, J = 8.1 Hz, 1H), 7.73 – 7.66 (m, 2H), 7.54 – 7.49 (m, 3H), 7.44 (t, J = 8.6 Hz, 3H), 6.43 (d, J = 16.0 Hz, 1H), 4.12 (s, 2H), 3.94 (s, 2H), 3.81 (s, 3H).

4.1.2. Methyl (*E*)-3-(4-((((6-chloroquinolin-2-yl)methyl)amino)methyl)phenyl)acrylate(**3b**)

Using the synthetic method for **3a**, the target compound was obtained as a yellow oil in 63% yield. ^{1}H NMR (400 MHz, $CDCl_3$) δ 8.05 (d, J = 8.5 Hz, 1H), 8.00 (d, J = 9.0 Hz, 1H), 7.79 (d, J = 2.3 Hz, 1H), 7.71 – 7.63 (m, 2H), 7.51 (d, J = 8.2 Hz, 2H), 7.48 – 7.42 (m, 3H), 6.42 (d, J = 16.0 Hz, 1H), 4.15 (s, 2H), 3.99 (s, 2H), 3.81 (s, 3H).

4.1.3. Methyl (*E*)-3-(4-((((6-bromoquinolin-2-yl)methyl)amino)methyl)phenyl)acrylate (**3c**)

Using the synthetic method for **3a**, the target compound was obtained as a yellow oil in 53% yield. ^{1}H NMR (400 MHz, $CDCl_3$) δ 8.04 (d, J = 8.5 Hz, 1H), 7.97 (d, J = 2.1 Hz, 1H), 7.93 (d, J = 8.9 Hz, 1H), 7.77 (dd, J = 9.0, 2.2 Hz, 1H), 7.68 (d, J = 16.0 Hz, 1H), 7.51 (d, J = 8.2 Hz, 2H), 7.48 – 7.43 (m, 3H), 6.43 (d, J = 16.0 Hz, 1H), 4.14 (s, 2H), 3.98 (s, 2H), 3.81 (s, 3H).

4.1.4. Methyl (*E*)-3-(4-((((6-methoxyquinolin-2-yl)methyl)amino)methyl)phenyl)acrylate(**3d**)

Using the synthetic method for **3a**, the target compound was obtained as a yellow oil in 39% yield. ^{1}H NMR (400 MHz, $CDCl_3$) δ 8.01 (d, J = 8.4 Hz, 1H), 7.95 (d, J = 9.2 Hz, 1H), 7.69 (d, J = 16.0 Hz, 1H), 7.49 (t, J = 8.3 Hz, 2H), 7.42 (t, J = 8.0 Hz, 2H), 7.40 – 7.33 (m, 2H), 7.07 (d, J = 2.7 Hz, 1H), 6.42 (d, J = 16.0 Hz, 1H), 4.60 (s, 2H), 4.08 (s, 2H), 3.93 (s, 3H), 3.81 (s, 3H).

4.1.5. Methyl (*E*)-3-(4-((((8-chloroquinolin-2-yl)methyl)amino)methyl)phenyl)acrylate (**3e**)

Using the synthetic method for **3a**, the target compound was obtained as a yellow oil in 62% yield. ^{1}H NMR (400 MHz, $CDCl_3$) δ 8.12 (d, J = 8.4 Hz, 1H), 7.82 (d, 1H), 7.71 (dd, J = 14.3, 12.2 Hz, 2H), 7.53 – 7.40 (m, 6H), 6.43 (d, J = 16.0 Hz, 1H), 4.16 (s, 2H), 3.96 (s, 2H), 3.80 (s, 3H).

4.1.6. Methyl (*E*)-3-(4-((((8-methoxyquinolin-2-yl)methyl)amino)methyl)phenyl)acrylate(**3f**)

Using the synthetic method for **3a**, the target compound was obtained as a yellow oil in 49% yield. ^{1}H NMR (400 MHz, $CDCl_3$) δ 8.10 (d, J = 8.5 Hz, 1H), 7.69 (d, J = 16.0 Hz, 1H), 7.57 (d, J = 8.4 Hz, 1H), 7.49 (d, J = 8.2 Hz, 2H), 7.44 – 7.40 (m, 3H), 7.38 (m, 1H), 7.05 (d, J = 7.5, 1.1 Hz, 1H), 6.42 (d, J = 16.0 Hz, 1H), 4.16 (s, 2H), 4.07 (s, 3H), 3.91 (s, 2H), 3.80 (s, 3H).

4.1.7. (*E*)-*N*-hydroxy-3-(4-(((quinolin-2-ylmethyl)amino)methyl)phenyl)acrylamide (**4a**)

Preparation of hydroxylamine in methanol:

Solution A was obtained by hydroxylamine hydrochloride (4.67g, 67 mmol) dissolving in methanol (24 ml). Solution B was acquired by potassium hydroxide (6.60 g, 100 mmol) diluting in methanol (14 ml). Next, solution B was added dropwise to the solution A at 0 °C. The reaction mixture was stirred for 30 min at 0 °C and filtered to give the solution C.

Compound **3a** (0.33g) was dissolved in the solution C (12 mL), and the reaction was stirred at RT for 4 h. Then the mixture was neutralized with 1 M HCl to Ph 7. White precipitate obtained was filtered and recrystallization to obtain a white solid (0.15g, 45%). mp：202-203 °C. ^{1}H NMR (400 MHz, DMSO) δ 10.90 (s, 1H), 9.84 (s, 1H), 9.10 (s, 1H), 8.46 (d, J = 8.5 Hz, 1H), 8.08 (d, J = 8.4 Hz, 1H), 8.04 (d, J = 8.0 Hz, 1H), 7.84 (dd, J = 11.2, 4.1 Hz, 1H), 7.71 – 7.61 (m, 6H), 7.49 (d, J = 15.8 Hz, 1H), 6.55 (d, J = 15.8 Hz, 1H), 4.52 (s, 2H), 4.34 (s, 2H). ^{13}C NMR (101 MHz, DMSO) δ 163.02, 153.45, 147.00, 137.89, 137.68, 135.95, 133.52, 131.41, 130.68, 128.87, 128.57, 128.04, 127.69, 127.45, 121.20, 120.71, 50.51, 50.25. HRMS (AP-ESI) m/z Calcd for $C_{20}H_{19}N_3O_2$ $[M+H]^+$ 334.155, found: 334.1560.

4.1.8.(*E*)-3-(4-((((6-chloroquinolin-2-yl)methyl)amino)methyl)phenyl)-*N*-hydroxyacrylamide (**4b**)

Using the synthetic method for **4a**, the target compound was obtained as a white solid in 29% yield. mp：202-205 °C. ^{1}H NMR (400 MHz, DMSO) δ 10.99 (s, 1H), 10.02 (s, 2H), 9.10 (s, 1H), 8.44 (d, J = 8.6 Hz, 1H), 8.19 (d, J = 2.4 Hz, 1H), 8.08 (d, J = 9.0 Hz, 1H), 7.84 (dd, J = 9.0, 2.4 Hz, 1H), 7.75 (d, J = 8.6 Hz, 1H), 7.68 (d, J = 8.2 Hz, 2H), 7.62 (d, J = 8.2 Hz, 2H), 7.48 (d, J = 15.8 Hz, 1H), 6.61 (d, J = 15.9 Hz, 1H), 4.49 (s, 2H), 4.32 (s, 2H). ^{13}C NMR (101 MHz, DMSO) δ 163.06, 155.21, 152.97, 138.88, 138.02, 137.40, 135.72, 134.89, 131.16, 128.74, 128.05, 127.67, 121.62, 120.43, 119.94, 109.56, 56.15, 51.22, 50.73. HRMS (AP-ESI) m/z Calcd for $C_{20}H_{18}ClN_3O_2$ $[M+H]^+$ 368.116, found: 368.1171.

4.1.9.(*E*)-3-(4-((((6-bromoquinolin-2-yl)methyl)amino)methyl)phenyl)-*N*-hydroxyacrylamide (**4c**)

Using the synthetic method for **4a**, the target compound was obtained as a white solid in 31% yield. mp：144-146 °C. ^{1}H NMR (400 MHz, DMSO) δ 10.86 (s, 1H), 9.07 (s, 1H), 8.43 (d, J = 8.6 Hz, 1H), 8.35 (d, J = 2.0 Hz, 1H), 8.01 (d, J = 9.0 Hz, 1H), 7.95 (dd, J = 9.0, 2.1 Hz, 1H), 7.69 (d, J = 8.6 Hz, 1H), 7.61 (d, J = 12.2 Hz, 4H), 7.48 (d, J = 15.9 Hz, 1H), 6.53 (d, J = 15.8 Hz, 1H), 4.47 (s, 2H), 4.29 (s, 2H). ^{13}C NMR (101 MHz, DMSO) δ 163.00, 154.80, 145.64, 143.66, 137.95, 136.84, 135.81, 133.66, 131.23, 131.15, 131.08, 130.55, 128.98, 128.78, 128.04, 122.17, 120.56, 120.26, 50.77, 50.44. HRMS (AP-ESI) m/z Calcd for $C_{20}H_{18}BrN_3O_2$ $[M+H]^+$ 412.0655, found: 412.0655.

4.1.10 (*E*)-*N*-hydroxy-3-(4-((((6-methoxyquinolin-2-yl)methyl)amino)methyl)phenyl)acrylamide (**4d**)

Using the synthetic method for **4a**, the target compound was obtained as a white solid in 34% yield. mp：148-151 °C. ^{1}H NMR (400 MHz, DMSO) δ 10.90 (s, 1H), 9.08 (s, 1H), 8.31 (d, J = 8.5 Hz, 1H), 7.94 (d, J = 9.1 Hz, 1H), 7.65 – 7.55 (m, 5H), 7.51 – 7.39 (m, 3H), 6.55 (d, J = 15.8 Hz, 1H), 4.31 (s, 2H), 4.18 (s, 2H), 3.91 (s, 3H). ^{13}C NMR (101 MHz, DMSO) δ 163.03, 157.84, 152.64, 143.14, 138.01, 136.26, 135.78, 135.41, 130.79, 130.33, 128.80, 127.99, 122.82, 121.46, 120.30, 106.30, 56.03, 51.52, 50.82. HRMS (AP-ESI) m/z Calcd for $C_{21}H_{21}N_3O_3$ $[M+H]^+$ 364.1656, found: 364.1656.

4.1.11(*E*)-3-(4-((((8-chloroquinolin-2-yl)methyl)amino)methyl)phenyl)-*N*-hydroxyacrylamide (**4e**)

Using the synthetic method for **4a**, the target compound was obtained as a white solid in 26% yield. mp：159-161 °C. ^{1}H NMR (400 MHz, DMSO) δ 10.87 (s, 1H), 9.07 (s, 1H), 8.54 (d, J = 8.5 Hz, 1H), 8.06 – 8.00 (m, 2H), 7.80 (d, J = 8.5 Hz, 1H), 7.66 – 7.59 (m, 5H), 7.48 (d, J = 15.8 Hz, 1H), 6.55 (d, J = 15.8 Hz, 1H), 4.52 (s, 2H), 4.38 (s, 2H). ^{13}C NMR (101 MHz, DMSO) δ 163.04, 155.42, 142.95, 138.27, 137.95, 135.74, 134.57, 132.32, 131.12, 130.67, 129.12, 128.80, 128.03, 127.64, 122.27, 120.50, 50.98, 50.65. HRMS (AP-ESI) m/z Calcd for $C_{20}H_{18}ClN_3O_2$ $[M+H]^+$ 368.116, found: 368.1161.

4.1.12 (*E*)-N-hydroxy-3-(4-((((8-methoxyquinolin-2-yl)methyl)amino)methyl)phenyl)acrylamide (**4f**)

Using the synthetic method for **4a**, the target compound was obtained as a white solid in 29% yield. mp：151-154 °C. ^{1}H NMR (400 MHz, DMSO) δ 10.82 (s, 1H), 9.07 (s, 1H), 8.39 (d, J = 8.5 Hz, 1H), 7.67 – 7.59 (m, 5H), 7.56 (d, J = 6.7 Hz, 2H), 7.52 (d, J = 7.7 Hz, 1H), 7.46 (d, J = 9.8 Hz, 1H), 7.29 (dd, J = 6.8, 2.2 Hz, 1H), 6.53 (d, J = 15.9 Hz, 1H), 4.45 (s, 2H), 4.28 (s, 2H), 4.02 (s, 3H). ^{13}C NMR (101 MHz, DMSO) δ 163.06, 155.21, 152.97, 138.88, 138.02, 137.40, 135.72, 134.89, 131.16, 128.74, 128.05, 127.67, 121.62, 120.43, 119.94, 109.56, 56.15, 51.22, 50.73. HRMS (AP-ESI) m/z Calcd for $C_{21}H_{21}N_3O_3$ $[M+H]^+$ 364.1656, found: 364.1656.

4.1.13 (*E*)-3-(3-((((6-bromoquinolin-2-yl)methyl)amino)methyl)phenyl)-*N*-hydroxyacrylamide (**4g**)

Using the synthetic method for **4a**, the target compound was obtained as a white solid in 36% yield. mp：176-178 °C. ^{1}H NMR (400 MHz, DMSO) δ 10.75 (s, 1H), 9.06 (s, 1H), 8.32 (d, J = 8.5 Hz, 1H), 8.26 (d, J = 2.1 Hz, 1H), 7.91 (d, J = 9.0 Hz, 1H), 7.84 (dd, J = 8.9, 2.2 Hz, 1H), 7.73 (d, J = 8.5 Hz, 1H), 7.58 (s, 1H), 7.47 – 7.32 (m, 4H), 6.47 (d, J = 15.8 Hz, 1H), 3.97 (s, 2H), 3.78 (s, 2H). ^{13}C NMR (101 MHz, DMSO) δ 163.17, 162.42, 146.06, 141.85, 138.85, 136.00, 135.18, 132.90, 131.13, 130.26, 129.70, 129.23, 128.75, 127.27, 126.59, 121.95, 119.46, 119.22, 54.95, 52.78. HRMS (AP-ESI) m/z Calcd for $C_{20}H_{18}BrN_3O_2$ $[M+H]^+$ 412.0655, found: 412.0667.

4.1.14 Methyl (*E*)-3-(4-((benzyl(quinolin-2-ylmethyl)amino)methyl)phenyl)acrylate (**5a**)

Compound **4a**(0.60g, 1.7mmol), Benzyl bromide (0.29g, 1.7mmol) and DIEA(3 equiv) was dissolved in DMSO (10 ml) and stirred for 4h at 50 °C. After cooled down, the mixture was poured into 100 ml H_2O and extracted with DCM. The solution was evaporated under vacuum to yield an oil (48%). The oil was purified by column chromatography (DCM/ MeOH 90:1).

^{1}H NMR (400 MHz, DMSO) δ 8.36 (d, J = 8.5 Hz, 1H), 8.01 (d, J = 8.4 Hz, 1H), 7.95 (d, J = 7.5 Hz, 1H), 7.77 – 7.64 (m, 5H), 7.58 (t, 1H), 7.49 (d, J = 8.1 Hz, 2H), 7.44 (d, J = 7.2 Hz, 2H), 7.37 (t, J = 7.5 Hz, 2H), 7.27 (t, J = 7.3 Hz, 1H), 6.63 (d, J = 16.1 Hz, 1H), 3.82 (s, 2H), 3.75 (s, 3H), 3.62 (s, 2H), 3.61 (s, 2H).

4.1.15 Methyl (*E*)-3-(4-((benzyl((6-chloroquinolin-2-yl)methyl)amino)methyl)phenyl)acrylate (**5b**)

Using the synthetic method for **5a**, the target compound was obtained as a light yellow oil in 56% yield. ^{1}H NMR (400 MHz, $CDCl_3$) δ 8.02 (d, J = 8.5 Hz, 1H), 7.96 (d, J = 9.0 Hz, 1H), 7.77 – 7.71 (m, 2H), 7.67 (d, J = 16.0 Hz, 1H), 7.60 (dd, J = 9.0, 2.3 Hz, 1H), 7.47 (d, J = 8.2 Hz, 2H), 7.45 – 7.38 (m, 4H), 7.33 (t, J = 7.5 Hz, 2H), 7.27 – 7.21 (m, 1H), 6.41 (d, J = 16.0 Hz, 1H), 3.87 (s, 2H), 3.79 (s, 3H), 3.64 (s, 2H), 3.64 (s, 2H).

4.1.16 Methyl (*E*)-3-(4-((benzyl((6-bromoquinolin-2-yl)methyl)amino)methyl)phenyl)acrylate (**5c**)

Using the synthetic method for **5a**, the target compound was obtained as a light yellow oil in 59% yield. ^{1}H NMR (400 MHz, DMSO) δ 8.36 – 8.30 (m, 2H), 8.22 (d, J = 2.2 Hz, 1H), 7.92 (d, J = 9.0 Hz, 1H), 7.83 (dd, J = 9.0, 2.2 Hz, 1H), 7.76 (d, J = 8.5 Hz, 1H), 7.72 – 7.62 (m, 3H), 7.47 (d, J = 8.1 Hz, 2H), 7.43 (d, J = 7.2 Hz, 2H), 7.36 (t, J = 7.5 Hz, 2H), 7.26 (t, J = 7.3 Hz, 1H), 6.61 (d, J = 16.1 Hz, 1H), 3.80 (s, 2H), 3.75 (s, 3H), 3.61 (s, 2H), 3.60 (s, 2H).

4.1.17 Methyl (*E*)-3-(4-((benzyl((6-methoxyquinolin-2-yl)methyl)amino)methyl)phenyl)acrylate (**5d**)

Using the synthetic method for **5a**, the target compound was obtained as a light yellow oil in 47% yield. ^{1}H NMR (400 MHz, CDCl3) δ 8.02 (d, J = 8.5 Hz, 1H), 7.94 (d, J = 9.2 Hz, 1H), 7.71 – 7.63 (m, 2H), 7.47 (d, J = 8.3 Hz, 2H), 7.45 – 7.37 (m, 4H), 7.36 – 7.30 (m, 3H), 7.26 – 7.21 (m, 1H), 7.05 (d, J = 2.7 Hz, 1H), 6.41 (d, J = 16.0 Hz, 1H), 3.90 (s, 3H), 3.86 (s, 2H), 3.79 (s, 3H), 3.63 (s, 4H).

4.1.18 Methyl (*E*)-3-(4-((((6-bromoquinolin-2-yl)methyl)(hexyl)amino)methyl)phenyl)acrylate (**5e**)

Using the synthetic method for **5a**, the target compound was obtained as a light yellow oil in 46% yield. ^{1}H NMR (400 MHz, DMSO) δ 8.29 (d, J = 8.6 Hz, 1H), 8.20 (d, J = 2.0 Hz, 1H), 7.88 (d, J = 9.0 Hz, 1H), 7.80 (dd, J = 8.9, 2.1 Hz, 1H), 7.68 (d, J = 8.5 Hz, 1H), 7.66 – 7.59 (m, 3H), 7.39 (d, J = 8.1 Hz, 2H), 6.58 (d, J = 16.0 Hz, 1H), 3.77 (s, 2H), 3.71 (s, 3H), 3.59 (s, 2H), 2.37 (t, J = 7.1 Hz, 2H), 1.47 – 1.37 (m, 2H), 1.19 – 1.08 (m, 4H), 1.08 – 0.98 (m, 2H), 0.73 (t, J = 7.2 Hz, 3H).

4.1.19 (*E*)-3-(4-((benzyl(quinolin-2-ylmethyl)amino)methyl)phenyl)-*N*-hydroxyacrylamide (**6a**)

Using the synthetic method for **4a**, the target compound was obtained as a white solid in 17% yield. mp：100-103 °C. ^{1}H NMR (400 MHz, DMSO) δ 10.73 (s, 1H), 9.01 (s, 1H), 8.36 (d, J = 8.4 Hz, 1H), 7.97 (d, J = 8.5 Hz, 1H), 7.94 (d, J = 7.9 Hz, 1H), 7.76 – 7.69 (m, 2H), 7.60 – 7.51 (m, 3H), 7.49 – 7.40 (m, 5H), 7.35 (t, J = 7.5 Hz, 2H), 7.26 (t, J = 7.3 Hz, 1H), 6.43 (d, J = 15.9 Hz, 1H), 3.81 (s, 2H), 3.61 (s, 2H), 3.60 (s, 2H). ^{13}C NMR (101 MHz, $CDCl_3$) δ 160.69, 147.02, 141.03, 138.82, 136.86, 133.39, 129.71, 129.17, 128.83, 128.32, 127.86, 127.58, 127.39, 127.12, 126.32, 120.90, 60.08, 58.41, 57.97. HRMS (AP-ESI) m/z Calcd for $C_{27}H_{25}N_3O_2$ $[M+H]^+$ 424.2020, found: 424.2029.

4.1.20

(*E*)-3-(4-((benzyl((6-chloroquinolin-2-yl)methyl)amino)methyl)phenyl)-*N*-hydroxyacrylamide (**6b**)

Using the synthetic method for **4a**, the target compound was obtained as a white solid in 26% yield. mp：110-112 °C. ^{1}H NMR (400 MHz, DMSO) δ 8.34 (d, J = 8.5 Hz, 1H), 8.09 (d, J = 2.3 Hz, 1H), 7.99 (d, J = 9.0 Hz, 1H), 7.77 (d, J = 8.6 Hz, 1H), 7.73 (dd, J = 9.0, 2.4 Hz, 1H), 7.50 (d, J = 8.0 Hz, 2H), 7.43 (d, J = 8.6 Hz, 4H), 7.37 – 7.31 (m, 3H), 7.28 – 7.23 (m, 1H), 6.41 (d, J = 15.8 Hz, 1H), 3.80 (s, 2H), 3.59 (s, 4H). ^{13}C NMR (101 MHz, DMSO) δ 163.26, 161.24, 145.82, 140.81, 139.07, 138.57, 136.34, 134.16, 131.09, 130.94, 130.40, 129.64, 129.13, 128.78, 128.23, 127.98, 127.54, 126.97, 122.16, 119.16, 59.88, 57.88, 57.53. HRMS (AP-ESI) m/z Calcd for $C_{27}H_{24}ClN_3O_2$ $[M+H]^+$ 458.1630, found: 458.1637.

4.1.21

(*E*)-3-(4-((benzyl((6-bromoquinolin-2-yl)methyl)amino)methyl)phenyl)-*N*-hydroxyacrylamide (**6c**)

Using the synthetic method for **4a**, the target compound was obtained as a white solid in 31% yield. mp：117-119 °C. ^{1}H NMR (400 MHz, DMSO) δ 10.73 (s, 1H), 9.04 (s, 1H), 8.35 (d, J = 8.5 Hz, 1H), 8.25 (d, J = 1.7 Hz, 1H), 7.92 (d, J = 9.0 Hz, 1H), 7.84 (dd, J = 9.0, 2.0 Hz, 1H), 7.77 (d, J = 8.5 Hz, 1H), 7.54 (d, J = 7.9 Hz, 2H), 7.49 – 7.40 (m, 5H), 7.35 (t, J = 7.5 Hz, 2H), 7.25 (t, J = 7.2 Hz, 1H), 6.43 (d, J = 15.9 Hz, 1H), 3.79 (s, 2H), 3.61 (s, 2H), 3.60 (s, 2H).^{13}C NMR (101 MHz, $CDCl_3$) δ 165.33, 161.19, 145.64, 140.93, 138.66, 135.68, 133.40, 132.99, 130.18, 129.57, 129.20, 128.83, 128.44, 128.36, 127.89, 127.20, 121.73, 120.05, 116.15, 60.01, 58.45, 58.01. HRMS (AP-ESI) m/z Calcd for $C_{27}H_{24}BrN_3O_2$ $[M+H]^+$ 502.1125, found: 502.1123.

4.1.22(*E*)-3-(4-((benzyl((6-methoxyquinolin-2-yl)methyl)amino)methyl)phenyl)-*N*-hydroxyacrylamide (**6d**)

Using the synthetic method for **4a**, the target compound was obtained as a white solid in 29% yield. mp：94-96 °C. ^{1}H NMR (400 MHz, DMSO) δ 10.75 (s, 1H), 9.02 (s, 1H), 8.25 (d, J = 8.5 Hz, 1H), 7.88 (d, J = 8.9 Hz, 1H), 7.66 (d, J = 8.5 Hz, 1H), 7.54 (d, J = 8.0 Hz, 2H), 7.44 (dd, J = 13.0, 7.5 Hz, 5H), 7.40 – 7.31 (m, 4H), 7.26 (t, J = 7.3 Hz, 1H), 6.44 (d, J = 15.8 Hz, 1H), 3.88 (s, 3H), 3.76 (s, 2H), 3.59 (d, J = 2.7 Hz, 4H). ^{13}C NMR (101 MHz, $CDCl_3$) δ 164.69, 158.03, 157.55, 143.12, 141.06, 140.47, 139.00, 135.61, 133.56, 129.87, 129.14, 128.83, 128.36, 128.30, 127.81, 127.06, 122.06, 121.23, 116.78, 105.30, 60.05, 58.35, 57.95, 55.53. HRMS (AP-ESI) m/z Calcd for $C_{28}H_{27}N_3O_3$ $[M+H]^+$ 454.2125, found: 454.2122.

4.1.23

(*E*)-3-(4-((((6-bromoquinolin-2-yl)methyl)(hexyl)amino)methyl)phenyl)-*N*-hydroxyacrylamide (**6e**)

Using the synthetic method for **4a**, the target compound was obtained as a white solid in 37% yield. mp：82-84 °C. ^{1}H NMR (400 MHz, DMSO) δ 10.75 (s, 1H), 9.03 (s, 1H), 8.33 (d, J = 8.6 Hz, 1H), 8.24 (d, J = 2.1 Hz, 1H), 7.91 (d, J = 9.0 Hz, 1H), 7.84 (dd, J = 9.0, 2.2 Hz, 1H), 7.72 (d, J = 8.5 Hz, 1H), 7.52 (d, J = 8.0 Hz, 2H), 7.47 – 7.38 (m, 3H), 6.44 (d, J = 15.8 Hz, 1H), 3.81 (s, 2H), 3.62 (s, 2H), 2.42 (t, J = 7.0 Hz, 2H), 1.52 – 1.40 (m, 2H), 1.18 (dt, J = 14.3, 7.2 Hz, 4H), 1.12 – 1.03 (m, 2H), 0.76 (t, J = 7.2 Hz, 3H). ^{13}C NMR (101 MHz, $CDCl_3$) δ 161.04, 148.30,

145.76, 140.70, 135.51, 133.60, 132.89, 130.35, 129.56, 129.32, 128.46, 127.93, 121.91, 120.34, 119.98, 116.73, 60.37, 58.43, 54.20, 31.59, 29.70, 26.88, 22.57, 14.02. HRMS (AP-ESI) m/z Calcd for $C_{26}H_{30}BrN_3O_2$ $[M+H]^+$ 496.1597, found: 496.1604.

4.1.24

(*E*)-3-(3-((benzyl((6-bromoquinolin-2-yl)methyl)amino)methyl)phenyl)-*N*-hydroxyacrylamide (**6f**)

Using the synthetic method for **4a**, the target compound was obtained as a white solid in 33% yield. mp：82-84 °C. ^{1}H NMR (400 MHz, DMSO) δ 10.82 (s, 1H), 9.10 (s, 1H), 8.33 (d, J = 9.1 Hz, 1H), 8.22 (d, J = 2.1 Hz, 1H), 7.90 (d, J = 9.0 Hz, 1H), 7.82 (dd, J = 9.0, 2.2 Hz, 1H), 7.77 (d, J = 8.6 Hz, 1H), 7.60 (s, 1H), 7.48(d, J = 15.8 Hz, 1H), 7.46 – 7.31 (m, 7H), 7.25 (t, J = 7.3 Hz, 1H), 6.49 (d, J = 15.8 Hz, 1H), 3.79 (s, 2H), 3.59 (s, 4H). ^{13}C NMR (101 MHz, $CDCl_3$) δ 165.26, 161.31, 145.42, 141.14, 139.45, 138.70, 135.73, 134.54, 132.97, 130.24, 129.94, 129.55, 128.85, 128.68, 128.40, 128.35, 127.17, 126.74, 121.80, 120.03, 116.93, 60.01, 58.63, 58.19.
HRMS (AP-ESI) m/z Calcd for $C_{27}H_{24}BrN_3O_2$ $[M+H]^+$ 502.1125, found: 502.1135.

4.1.25

(*E*)-3-(3-((((6-bromoquinolin-2-yl)methyl)(hexyl)amino)methyl)phenyl)-*N*-hydroxyacrylamide (**6g**)

Using the synthetic method for **4a**, the target compound was obtained as a white solid in 26% yield. mp：76-78 °C. ^{1}H NMR (400 MHz, DMSO) δ 10.75 (s, 1H), 9.11 (s, 1H), 8.33 (d, J = 8.5 Hz, 1H), 8.24 (d, J = 1.7 Hz, 1H), 7.91 (d, J = 9.0 Hz, 1H), 7.84 (dd, J = 8.9, 2.0 Hz, 1H), 7.73 (d, J = 8.5 Hz, 1H), 7.56 (s, 1H), 7.51 – 7.31 (m, 4H), 6.48 (d, J = 15.8 Hz, 1H), 3.82 (s, 2H), 3.63 (s, 2H), 2.43 (t, J = 6.9 Hz, 2H), 1.51 – 1.44 (m, 2H), 1.22 – 1.14 (m, 4H), 1.11 – 1.04 (m, 2H), 0.76 (t, J = 9.4, 5.0 Hz, 3H). ^{13}C NMR (101 MHz, $CDCl_3$) δ 164.82, 161.37, 145.63, 140.98, 139.50, 135.60, 134.64, 132.94, 130.41, 130.14, 129.58, 128.64, 128.46, 127.66, 126.80, 121.99, 120.00, 116.84, 60.46, 58.61, 54.38, 31.61, 29.72, 26.91, 22.59, 14.03. HRMS (AP-ESI) m/z Calcd for $C_{26}H_{30}BrN_3O_2$ $[M+H]^+$ 496.1594, found: 496.1604.

4.1.26 *N*-(quinolin-2-ylmethyl)aniline (**7a**)

Aldehyde **1a** (0.16g, 1 mmol) was dissolved in DCM (10 ml) and aniline (0.11g, 1.2 mmol) was added dropwise. The reaction was stirred at RT for overnight, and a crude product was obtained after evaporation of the solvent. Then MeOH and $NaBH_4$ (0.113 g, 3 mmol) was added, and reaction mixture was stirred 2h at RT. The mixture was concentrated under reduced pressure and added saturated $NaCO_3$ solution. The aqueous phase was extracted with EtOAc, dried over anhydrous $MgSO_4$ and evaporated to give crude residue. The crude product was purified by column chromatography (petroleum ether/EtOAc 30: 1). mp：56-58 °C.^{1}H NMR (400 MHz, $CDCl_3$) δ 8.12 (t, 2H), 7.82 (d, J = 8.3 Hz, 1H), 7.73 (t, 1H), 7.54 (t, 1H), 7.46 (d, 1H), 7.21 (t, J = 7.8 Hz, 2H), 6.74 (t, J = 8.7 Hz, 3H), 5.14 (s, 1H), 4.64 (d, J = 5.2 Hz, 2H).

4.1.27 4-Bromo-*N*-(quinolin-2-ylmethyl)aniline (**7b**)

Using the synthetic method for **7a**, the target compound was obtained as a white solid in 66% yield. mp：128-131 °C. ^{1}H NMR (400 MHz, $CDCl_3$) δ 8.11 (dd, J = 11.3, 8.6 Hz, 2H), 7.82 (d, J = 8.1 Hz, 1H), 7.74 (t, J = 7.6 Hz, 1H), 7.54 (t, J = 7.5 Hz, 1H), 7.41 (d, J = 8.4 Hz, 1H), 7.27 (d, J = 8.8 Hz, 2H), 6.63 (d, J = 8.7 Hz, 2H), 5.27 (s, 1H), 4.59 (d, J = 5.1 Hz, 2H).

4.1.28 4-Methoxy-*N*-(quinolin-2-ylmethyl)aniline (**7c**)

Using the synthetic method for **7a**, the target compound was obtained as a light yellow solid in 61% yield. mp：138-141 °C. ^{1}H NMR (400 MHz, $CDCl_3$) δ 8.11 (t, J = 7.6 Hz, 2H), 7.81 (d, J = 7.9 Hz, 1H), 7.73 (t, J = 7.8 Hz, 1H), 7.54 (d, J = 7.5 Hz, 1H), 7.46 (d, J = 8.5 Hz, 1H), 6.80 (d, J = 8.9 Hz, 2H), 6.71 (d, J = 8.9 Hz, 2H), 4.60 (s, 2H), 3.75 (s, 3H).

4.1.29 *N*-((8-chloroquinolin-2-yl)methyl)-4-methoxyaniline (**7d**)

Using the synthetic method for **7a**, the target compound was obtained as a white solid in 58% yield. ^{1}H NMR (400 MHz, $CDCl_3$) δ 8.14 (d, J = 8.5 Hz, 1H), 7.85 (d, J = 7.5, 1.1 Hz, 1H), 7.75 (d, 1H), 7.51 (d, J = 8.5 Hz, 1H), 7.47 (t, J = 7.8 Hz, 1H), 6.81 (d, J = 1.8 Hz, 4H), 4.68 (s, 2H), 3.75 (s, 3H).

4.1.30 *N*-((6-bromoquinolin-2-yl)methyl)aniline (**7e**)

Using the synthetic method for **7a**, the target compound was obtained as a white solid in 41% yield. mp：192-193°C.^{1}H NMR (400 MHz, $CDCl_3$) δ 8.06 – 7.95 (m, 3H), 7.79 (dd, J = 8.9, 2.2 Hz, 1H), 7.48 (d, J = 8.5 Hz, 1H), 7.20 (dd, J = 8.6, 7.3 Hz, 2H), 6.73 (d, J = 7.7 Hz, 3H), 4.62 (s, 2H).

4.1.31 *N*-((8-methoxyquinolin-2-yl)methyl)aniline(**7f**)

Using the synthetic method for **7a**, the target compound was obtained as a brown solid in 46% yield. ^{1}H NMR (400 MHz, $CDCl_3$) δ 8.09 (d, J = 8.5 Hz, 1H), 7.55 (d, J = 8.5 Hz, 1H), 7.44 (d, J = 7.8 Hz, 1H), 7.39 (d, J = 7.3 Hz, 1H), 7.21 – 7.14 (m, 2H), 7.09 (d, J = 7.5 Hz, 1H), 6.75 – 6.66 (m, 3H), 4.73 (s, 2H), 4.12 (s, 3H).

4.1.32 *N*-((6-methoxyquinolin-2-yl)methyl)aniline (**7g**)

Using the synthetic method for **7a**, the target compound was obtained as a pale yellow solid in 49% yield. ^{1}H NMR (400 MHz, $CDCl_3$) δ 8.04 (d, J = 8.4 Hz, 2H), 7.43 (d, J = 8.5 Hz, 1H), 7.39 (dd, J = 9.2, 2.8 Hz, 1H), 7.21 (d, J = 7.1 Hz, 1H), 7.18 (d, J = 7.4 Hz, 1H), 7.08 (d, J = 2.8 Hz, 1H), 6.73 (m, 3H), 4.62 (s, 2H), 3.94 (s, 3H).

4.1.33 Methyl (*E*)-3-(4-(phenyl(quinolin-2-ylmethyl)carbamoyl)phenyl)acrylate (**10a**)

Compound **9a** (0.82 g, 4 mmol) was dissolved in 20 mL DCM and one drop DMF was added. Then oxalyl chloride (1 mL, 12 mmol) was added dropwise and the reaction was stirred at RT for 1h. After the mixture was evaropated, the residue was dissolved in DCM and again concentrated in vacuo to offer quantitatively the crude chloride. A solution of chloride in DCM (20 mL) was suspended with $NaHCO_3$ (2.7 g) and compound **7a** (0.47g, 2mmol) was added dropwise with stirring. After the addition, the reaction was stirred for 4 h. Then the mixture was washed with 1M citric acid(×3), saturate solution of $NaHCO_3$(×3) and brine solution(×3). The solution was concentrated in vacuo, then purified via chlomatography on silica (petroleum ether / EtOAc=3:1) to give a white solid as the target compound（0.5g，50%）. mp：128-131 °C. ^{1}H NMR (400 MHz, $CDCl_3$) δ 8.16 (d, J = 8.5 Hz, 1H), 8.03 (d, J = 8.4 Hz, 1H), 7.81 (d, J = 8.1 Hz, 1H), 7.69 (t, J = 7.7 Hz, 1H), 7.61 (d, J = 3.8 Hz, 1H), 7.57 (d, J = 11.4 Hz, 1H), 7.52 (t, J = 7.5 Hz, 1H), 7.44 (d, J = 8.2 Hz, 2H), 7.35 (d, J = 8.2 Hz, 2H), 7.18 – 7.08 (m, 5H), 6.39 (d, J = 16.0 Hz, 1H), 5.45 (s,

2H), 3.79 (s, 3H).

4.1.34 Methyl (*E*)-3-(4-((4-bromophenyl)(quinolin-2-ylmethyl)carbamoyl)phenyl)acrylate (**10b**)

Using the synthetic method for **10a**, the target compound was obtained as a white solid in 33% yield. mp：178-180 °C. ^{1}H NMR (400 MHz, $CDCl_3$) δ 8.16 (d, J = 8.5 Hz, 1H), 8.02 (d, J = 8.4 Hz, 1H), 7.81 (d, J = 8.1 Hz, 1H), 7.73 – 7.68 (m, 1H), 7.62 (s, 1H), 7.56 (d, J = 8.4 Hz, 1H), 7.52 (d, 1H), 7.44 (d, J = 8.3 Hz, 2H), 7.38 (d, J = 8.3 Hz, 2H), 7.28 (d, J = 8.8 Hz, 2H), 7.03 (d, J = 8.7 Hz, 2H), 6.41 (d, J = 16.0 Hz, 1H), 5.40 (s, 2H), 3.80 (s, 3H).

4.1.35 Methyl (*E*)-3-(4-((4-methoxyphenyl)(quinolin-2-ylmethyl)carbamoyl)phenyl)acrylate (**10c**)

Using the synthetic method for **10a**, the target compound was obtained as a white solid in 44% yield. mp：158-160 °C. ^{1}H NMR (400 MHz, $CDCl_3$) δ 8.16 (d, J = 8.5 Hz, 1H), 8.03 (d, J = 8.4 Hz, 1H), 7.81 (d, J = 8.2 Hz, 1H), 7.69 (t, J = 7.1 Hz, 1H), 7.59 (d, J = 16.1 Hz, 2H), 7.52 (t, J = 7.1 Hz, 1H), 7.43 (d, J = 7.6 Hz, 2H), 7.35 (d, J = 8.2 Hz, 2H), 7.02 (d, J = 8.3 Hz, 2H), 6.65 (d, J = 8.7 Hz, 2H), 6.39 (d, J = 16.0 Hz, 1H), 5.41 (s, 2H), 3.79 (s, 3H), 3.69 (s, 3H).

4.1.36 Methyl (*E*)-3-(4-(((8-chloroquinolin-2-yl)methyl)(4-methoxyphenyl)carbamoyl)phenyl)acrylate (**10d**)

Using the synthetic method for **10a**, the target compound was obtained as a white solid in 62% yield. mp：170-172 °C. ^{1}H NMR (400 MHz, $CDCl_3$) δ 8.21 – 8.15 (m, 1H), 7.83 (d, J = 7.5 Hz, 1H), 7.74 (d, J = 8.1 Hz, 1H), 7.59 (d, J = 16.1 Hz, 2H), 7.48 – 7.41 (m, 3H), 7.34 (t, 4H), 6.71 (d, J = 8.7 Hz, 2H), 6.39 (d, J = 16.0 Hz, 1H), 5.44 (s, 2H), 3.79 (s, 3H), 3.72 (s, 3H).

4.1.37 Methyl (*E*)-3-(4-(((6-bromoquinolin-2-yl)methyl)(phenyl)carbamoyl)phenyl)acrylate (**10e**)

Using the synthetic method for **10a**, the target compound was obtained as a white solid in 57% yield. mp：175-177 °C. ^{1}H NMR (400 MHz, $CDCl_3$) δ 8.08 (d, J = 8.5 Hz, 1H), 8.00 – 7.87 (m, 2H), 7.75 (dd, J = 8.9, 2.1 Hz, 1H), 7.65 – 7.53 (m, 2H), 7.43 (d, J = 8.3 Hz, 2H), 7.34 (d, J = 8.3 Hz, 2H), 7.20 – 7.06 (m, 5H), 6.38 (d, J = 16.0 Hz, 1H), 5.43 (s, 2H), 3.78 (s, 3H).

4.1.38 Methyl (*E*)-3-(4-(((8-methoxyquinolin-2-yl)methyl)(phenyl)carbamoyl)phenyl)acrylate (**10f**)

Using the synthetic method for **10a**, the target compound was obtained as a white solid in 59% yield. mp：162-165 °C. ^{1}H NMR (400 MHz, $CDCl_3$) δ 8.18 (t, J = 7.6 Hz, 1H), 7.67 (d, J = 8.5 Hz, 1H), 7.58 (d, J = 16.0 Hz, 1H), 7.46 (d, 1H), 7.45 – 7.42 (m, 2H), 7.40 (d, J = 7.4 Hz, 1H), 7.35 (d, J = 8.3 Hz, 2H), 7.17 – 7.05 (m, 6H), 6.39 (d, J = 16.0 Hz, 1H), 5.61 (s, 2H), 4.07 (s, 3H), 3.79 (s, 3H).

4.1.39 Methyl (*E*)-3-(4-(2-oxo-2-(phenyl(quinolin-2-ylmethyl)amino)ethyl)phenyl)acrylate (**10g**)

Using the synthetic method for **10a**, the target compound was obtained as a white solid in 49%

yield. mp：168-170 °C. ^{1}H NMR (400 MHz, $CDCl_3$) δ 8.12 (d, J = 8.1 Hz, 1H), 7.98 (s, 1H), 7.79 (d, J = 8.0 Hz, 1H), 7.73 – 7.63 (m, 2H), 7.55 – 7.46 (m, 2H), 7.42 (d, J = 8.1 Hz, 2H), 7.34 – 7.28 (m, 3H), 7.15 (d, J = 7.7 Hz, 4H), 6.41 (d, J = 16.0 Hz, 1H), 5.23 (s, 2H), 3.81 (s, 3H), 3.59 (s, 2H).

4.1.40

Methyl(*E*)-3-(4-(2-(((6-bromoquinolin-2-yl)methyl)(phenyl)amino)-2-oxoethyl)phenyl)acrylate (**10h**)

Using the synthetic method for 10a, the target compound was obtained as a white solid in 44% yield. mp：162-164 °C.^{1}H NMR (400 MHz, $CDCl_3$) δ 8.05 (d, J = 8.4 Hz, 1H), 7.96 (d, J = 1.8 Hz, 1H), 7.87 (s, 1H), 7.75 (d, J = 8.9 Hz, 1H), 7.67 (d, J = 16.0 Hz, 1H), 7.52 (d, J = 8.5 Hz, 1H), 7.42 (d, J = 8.1 Hz, 2H), 7.37 – 7.29 (m, 3H), 7.20 – 7.08 (m, 4H), 6.41 (d, J = 16.0 Hz, 1H), 5.21 (s, 2H), 3.81 (s, 3H), 3.58 (s, 2H).

4.1.41

Methyl(*E*)-3-(4-(2-(((6-methoxyquinolin-2-yl)methyl)(phenyl)amino)-2-oxoethyl)phenyl)acrylate (**10i**)

Using the synthetic method for 10a, the target compound was obtained as a white solid in 55% yield. mp：172-174 °C. ^{1}H NMR (400 MHz, $CDCl_3$) δ 8.03 (d, J = 7.2 Hz, 1H), 7.88 (s, 1H), 7.67 (d, J = 16.0 Hz, 1H), 7.47 (d, J = 8.4 Hz, 1H), 7.42 (d, J = 8.1 Hz, 2H), 7.37 – 7.27 (m, 4H), 7.18 – 7.04 (m, 5H), 6.41 (d, J = 16.0 Hz, 1H), 5.21 (s, 2H), 3.92 (s, 3H), 3.81 (s, 3H), 3.58 (s, 2H).

4.1.42

(*E*)-4-(3-(hydroxyamino)-3-oxoprop-1-en-1-yl)-*N*-phenyl-*N*-(quinolin-2-ylmethyl)benzamide (**11a**)

Using the synthetic method for **4a**, the target compound was obtained as a white solid in 41% yield. mp：176-180 °C. ^{1}H NMR (300 MHz, DMSO) δ 10.75 (s, 1H), 9.05 (s, 1H), 8.36 (d, J = 8.5 Hz, 1H), 7.96 (dd, J = 8.1, 3.0 Hz, 2H), 7.78 – 7.70 (m, 1H), 7.63 (d, J = 8.5 Hz, 1H), 7.59 (dd, J = 11.0, 3.9 Hz, 1H), 7.48 – 7.39 (m, 4H), 7.35 (d, 1H), 7.22 (dt, J = 15.2, 7.6 Hz, 4H), 7.09 (t, J = 7.0 Hz, 1H), 6.43 (d, J = 15.9 Hz, 1H), 5.37 (s, 2H). ^{13}C NMR (101 MHz, DMSO) δ 169.85, 162.86, 158.14, 147.48, 143.85, 137.72, 137.28, 137.24, 136.35, 130.15, 129.45, 129.03, 128.31, 127.97, 127.39, 127.34, 127.06, 126.77, 120.97, 120.42, 55.89. HRMS (AP-ESI) m/z Calcd for $C_{26}H_{21}N_3O_3$ $[M+H]^+$ 424.1656, found: 424.1661.

4.1.43

(*E*)-*N*-(4-bromophenyl)-4-(3-(hydroxyamino)-3-oxoprop-1-en-1-yl)-*N*-(quinolin-2-ylmethyl)benzamide (**11b**)

Using the synthetic method for **4a**, the target compound was obtained as a white solid in 33% yield. mp：192-193 °C. ^{1}H NMR (400 MHz, DMSO) δ 10.77 (s, 1H), 9.07 (s, 1H), 8.36 (d, J = 8.5 Hz, 1H), 7.96 (dd, J = 7.7, 4.3 Hz, 2H), 7.78 – 7.72 (m, 1H), 7.61 (d, J = 8.3 Hz, 1H), 7.59 – 7.56 (m, 1H), 7.49 (d, J = 8.3 Hz, 2H), 7.46 – 7.35 (m, 6H), 7.23 (d, J = 8.7 Hz, 2H), 6.46 (d, J = 15.8 Hz, 1H), 5.36 (s, 2H). ^{13}C NMR (101 MHz, DMSO) δ 169.75, 162.89, 157.84, 147.48, 143.29, 137.65, 137.29, 136.95, 136.60, 132.33, 130.18, 130.01, 129.49, 129.05, 128.32, 127.48, 127.41,

126.81, 121.26, 120.43, 119.70, 55.66. HRMS (AP-ESI) m/z Calcd for $C_{26}H_{20}BrN_3O_3$ $[M+H]^+$ 502.0761, found: 502.0769.

4.1.44

(E)-4-(3-(hydroxyamino)-3-oxoprop-1-en-1-yl)-*N*-(4-methoxyphenyl)-*N*-(quinolin-2-ylmethyl)benzamide (**11c**)

Using the synthetic method for **4a**, the target compound was obtained as a white solid in 32% yield. mp：188-190 °C. ^{1}H NMR (400 MHz, DMSO) δ 10.78 (s, 1H), 9.08 (s, 1H), 8.36 (d, J = 8.5 Hz, 1H), 7.96 (dd, J = 7.7, 5.0 Hz, 2H), 7.77 – 7.71 (m, 1H), 7.64 (d, J = 8.4 Hz, 1H), 7.61 – 7.55 (m, 1H), 7.49 – 7.34 (m, 5H), 7.18 (d, J = 8.6 Hz, 2H), 6.74 (d, J = 8.8 Hz, 2H), 6.44 (d, J = 15.8 Hz, 1H), 5.32 (s, 2H), 3.62 (s, 3H). ^{13}C NMR (101 MHz, DMSO) δ 169.85, 162.92, 158.21, 157.99, 147.46, 137.72, 137.47, 137.22, 136.44, 136.17, 130.14, 129.38, 129.03, 128.31, 127.39, 127.31, 126.76, 121.01, 120.49, 114.59, 56.03, 55.57. HRMS (AP-ESI) m/z Calcd for $C_{27}H_{23}N_3O_4$ $[M+H]^+$ 454.1761, found: 454.1755.

4.1.45

(*E*)-*N*-((8-chloroquinolin-2-yl)methyl)-4-(3-(hydroxyamino)-3-oxoprop-1-en-1-yl)-*N*-(4-methoxyphenyl)benzamide (**11d**)

Using the synthetic method for **4a**, the target compound was obtained as a white solid in 54% yield. mp：178-179 °C. ^{1}H NMR (400 MHz, DMSO) δ 10.74 (s, 1H), 9.11 (s, 1H), 8.44 (d, J = 8.5 Hz, 1H), 8.02 – 7.91 (m, 2H), 7.71 (d, J = 8.3 Hz, 1H), 7.57 (t, J = 7.8 Hz, 1H), 7.50 – 7.28 (m, 7H), 6.77 (d, J = 8.9 Hz, 2H), 6.45 (d, J = 15.8 Hz, 1H), 5.34 (s, 2H), 3.64 (s, 3H). ^{13}C NMR (101 MHz, DMSO) δ 169.75, 162.86, 159.04, 158.05, 143.34, 137.78, 137.70, 137.61, 136.93, 136.08, 132.44, 130.23, 129.66, 129.25, 128.87, 127.87, 127.29, 126.95, 121.58, 120.88, 114.51, 55.59, 49.08. HRMS (AP-ESI) m/z Calcd for $C_{27}H_{22}ClN_3O_4$ $[M+H]^+$ 488.1372, found: 488.1364.

4.1.46

(*E*)-*N*-((6-bromoquinolin-2-yl)methyl)-4-(3-(hydroxyamino)-3-oxoprop-1-en-1-yl)-*N*-phenylbenzamide (**11e**)

Using the synthetic method for **4a**, the target compound was obtained as a white solid in 39% yield. mp：138-141 °C. ^{1}H NMR (400 MHz, DMSO) δ 10.73 (s, 1H), 9.04 (s, 1H), 8.35 (d, J = 8.6 Hz, 1H), 8.27 (s, 1H), 7.94 – 7.82 (m, 2H), 7.69 (d, J = 8.5 Hz, 1H), 7.48 – 7.32 (m, 5H), 7.28 – 7.15 (m, 4H), 7.10 (t, J = 7.2 Hz, 1H), 6.44 (d, J = 19.9 Hz, 1H), 5.35 (s, 2H). ^{13}C NMR (101 MHz, DMSO) δ 169.84, 162.90, 158.94, 146.08, 143.82, 137.77, 137.21, 136.50, 136.35, 133.17, 131.24, 130.32, 129.47, 128.73, 127.99, 127.33, 127.11, 121.41, 120.98, 119.59, 55.87. HRMS (AP-ESI) m/z Calcd for $C_{26}H_{20}BrN_3O_3$ $[M+H]^+$ 502.0761, found: 502.0772.

4.1.47

(*E*)-4-(3-(hydroxyamino)-3-oxoprop-1-en-1-yl)-*N*-((8-methoxyquinolin-2-yl)methyl)-*N*-phenylbenzamide (**11f**)

Using the synthetic method for **4a**, the target compound was obtained as a white solid in 29% yield. mp：198-200 °C. ^{1}H NMR (400 MHz, DMSO) δ 10.75 (s, 1H), 9.05 (s, 1H), 8.30 (d, J = 8.5 Hz, 1H), 7.63 (d, J = 8.5 Hz, 1H), 7.50 – 7.42 (m, 5H), 7.38 (d, J = 15.8 Hz, 1H), 7.28 (d, J = 7.7 Hz, 2H), 7.19 (dd, J = 9.4, 6.0 Hz, 3H), 7.09 (t, J = 7.4 Hz, 1H), 6.44 (d, J = 15.8 Hz, 1H), 5.35 (s,

2H), 3.96 (s, 3H). ^{13}C NMR (101 MHz, DMSO) δ 170.00, 162.94, 156.49, 155.38, 143.95, 139.28, 137.80, 137.54, 137.04, 136.23, 129.44, 129.38, 128.43, 128.06, 127.28, 127.01, 120.94, 120.59, 119.77, 109.23, 56.20, 55.90. HRMS (AP-ESI) m/z Calcd for $C_{27}H_{23}N_3O_4$ $[M+H]^+$ 454.1689, found: 454.1699.

4.1.48

(*E*)-N-hydroxy-3-(4-(2-oxo-2-(phenyl(quinolin-2-ylmethyl)amino)ethyl)phenyl)acrylamide (**11g**)

Using the synthetic method for **4a**, the target compound was obtained as a white solid in 37% yield. mp：160-164 °C. ^{1}H NMR (400 MHz, DMSO) δ 10.73 (s, 1H), 9.02 (s, 1H), 8.33 (d, J = 8.5 Hz, 1H), 7.98 – 7.88 (m, 2H), 7.74 (t, J = 7.5 Hz, 1H), 7.57 (t, J = 13.7, 5.9 Hz, 2H), 7.53 (d, J = 8.4 Hz, 1H), 7.46 (d, J = 8.3 Hz, 2H), 7.43 – 7.27 (m, 5H), 7.16 (d, J = 7.4 Hz, 2H), 6.42 (d, J = 15.8 Hz, 1H), 5.15 (s, 2H), 3.57 (s, 2H). ^{13}C NMR (101 MHz, DMSO) δ 170.50, 163.31, 158.18, 147.40, 143.09, 138.61, 137.76, 137.12, 133.50, 130.28, 130.13, 130.00, 128.95, 128.80, 128.39, 128.30, 127.75, 127.36, 126.74, 120.53, 119.08, 55.38. HRMS (AP-ESI) m/z Calcd for $C_{27}H_{23}N_3O_3$ $[M+H]^+$ 438.1812, found: 438.1816.

4.1.49

(*E*)-3-(4-(2-(((6-bromoquinolin-2-yl)methyl)(phenyl)amino)-2-oxoethyl)phenyl)-*N*-hydroxyacrylamide (**11h**)

Using the synthetic method for **4a**, the target compound was obtained as a white solid in 46% yield. mp：170-173 °C. ^{1}H NMR (400 MHz, DMSO) δ 8.33 (d, J = 8.6 Hz, 1H), 8.26 (s, 1H), 7.86 (d, J = 1.9 Hz, 2H), 7.59 (d, J = 8.5 Hz, 1H), 7.47 (d, J = 8.4 Hz, 2H), 7.44 – 7.29 (m, 6H), 7.17 (d, J = 7.6 Hz, 2H), 6.50 (d, J = 15.8 Hz, 1H), 5.15 (s, 2H), 3.58 (s, 2H). ^{13}C NMR (101 MHz, DMSO) δ 170.53, 163.20, 158.98, 146.00, 143.06, 138.32, 137.64, 136.39, 133.56, 133.16, 131.14, 130.30, 130.24, 130.01, 128.78, 128.69, 128.42, 127.71, 121.50, 119.56, 119.30, 55.36. HRMS (AP-ESI) m/z Calcd for $C_{27}H_{22}BrN_3O_3$ $[M+H]^+$ 516.0917, found: 516.0928.

4.1.50

(*E*)-*N*-hydroxy-3-(4-(2-(((6-methoxyquinolin-2-yl)methyl)(phenyl)amino)-2-oxoethyl)phenyl)acrylamide (**11i**)

Using the synthetic method for **4a**, the target compound was obtained as a white solid in 33% yield. mp：190-191 °C. ^{1}H NMR (400 MHz, DMSO) δ 10.77 (s, 1H), 9.04 (s, 1H), 8.22 (d, J = 8.5 Hz, 1H), 7.82 (d, J = 8.9 Hz, 1H), 7.54 – 7.43 (m, 3H), 7.43 – 7.26 (m, 8H), 7.16 (d, J = 7.2 Hz, 2H), 6.45 (d, J = 15.8 Hz, 1H), 5.11 (s, 2H), 3.88 (s, 3H), 3.56 (s, 2H). ^{13}C NMR (101 MHz, DMSO) δ 170.46, 168.12, 163.34, 157.56, 155.43, 143.31, 143.03, 138.54, 137.75, 136.03, 133.53, 130.31, 130.27, 129.97, 128.80, 128.42, 127.74, 122.43, 120.79, 119.20, 106.18, 55.95, 55.16. HRMS (AP-ESI) m/z Calcd for $C_{28}H_{25}N_3O_4$ $[M+H]^+$ 468.1918, found: 468.1926.

4.1.51 Methyl 4-(((quinolin-2-ylmethyl)amino)methyl)benzoate (**13a**)

Using the synthetic method for **4a**, the target compound was obtained as a yellow oil in 40% yield. ^{1}H NMR (400 MHz, $CDCl_3$) δ 8.11 (d, J = 8.4 Hz, 1H), 8.06 (d, J = 8.5 Hz, 1H), 8.01 (d, J = 8.3 Hz, 2H), 7.80 (d, J = 8.1 Hz, 1H), 7.73 – 7.67 (m, 1H), 7.52 (t, J = 11.6, 4.6 Hz, 1H), 7.48 (d, J = 8.3 Hz, 2H), 7.44 (d, J = 8.4 Hz, 1H), 4.11 (s, 2H), 3.97 (s, 2H), 3.91 (s, 3H).

4.1.52 Methyl 4-((((8-chloroquinolin-2-yl)methyl)amino)methyl)benzoate (**13b**)

Using the synthetic method for **4a**, the target compound was obtained as a yellow oil in 37%. ^{1}H NMR (400 MHz, $CDCl_3$) δ 7.91 (d, J = 8.2 Hz, 3H), 7.85 – 7.80 (m, 2H), 7.65 (dd, J = 9.0, 2.2 Hz, 1H), 7.36 (t, J = 8.3 Hz, 3H), 3.99 (s, 2H), 3.87 (s, 2H), 3.81 (s, 3H).

4.1.53 Methyl 4-((((6-bromoquinolin-2-yl)methyl)amino)methyl)benzoate(**13c**)

Using the synthetic method for **4a**, the target compound was obtained as a yellow oil in 53% yield. ^{1}H NMR (400 MHz, $CDCl_3$) δ 8.01 (d, J = 8.2 Hz, 3H), 7.94 (d, J = 2.1 Hz, 1H), 7.92 (d, J = 9.0 Hz, 1H), 7.75 (dd, J = 9.0, 2.2 Hz, 1H), 7.46 (t, J = 8.3 Hz, 3H), 4.09 (s, 2H), 3.97 (s, 2H), 3.91 (s, 3H).

4.1.54 Methyl 4-((((6-methoxyquinolin-2-yl)methyl)amino)methyl)benzoate(**13d**)

Using the synthetic method for **4a**, the target compound was obtained as a yellow oil in 44% yield. ^{1}H NMR (400 MHz, $CDCl_3$) δ 7.99 (d, J = 8.2 Hz, 2H), 7.94 (d, 2H), 7.44 (d, J = 8.1 Hz, 2H), 7.37 – 7.31 (m, 2H), 7.01 (d, J = 2.6 Hz, 1H), 4.04 (s, 2H), 3.91 (s, 2H), 3.87 (s, 3H), 3.86 (s, 3H).

4.1.55 Methyl 4-((benzyl(quinolin-2-ylmethyl)amino)methyl)benzoate (**15a**)

Using the synthetic method for **5a**, the target compound was obtained as a colourless oil in 33% yield. ^{1}H NMR (400 MHz, $CDCl_3$) δ 8.13 (d, J = 8.5 Hz, 1H), 8.04 (d, J = 8.5 Hz, 1H), 7.99 (d, J = 8.3 Hz, 2H), 7.79 (d, J = 8.1 Hz, 1H), 7.72 (d, J = 8.5 Hz, 1H), 7.71 – 7.65 (m, 1H), 7.54 – 7.47 (m, 3H), 7.41 (d, J = 7.1 Hz, 2H), 7.33 (t, J = 7.4 Hz, 2H), 7.23 (d, 1H), 3.90 (s, 3H), 3.89 (s, 2H), 3.69 (s, 2H), 3.64 (s, 2H).

4.1.56 *N*-hydroxy-4-(((quinolin-2-ylmethyl)amino)methyl)benzamide (**14a**)

Using the synthetic method for **6a**, the target compound was obtained as a white solid in 44% yield. mp：186-188 °C. ^{1}H NMR (400 MHz, DMSO) δ 11.32 (s, 1H), 9.69 (s, 1H), 9.12 (s, 1H), 8.47 (d, J = 8.5 Hz, 1H), 8.09 (d, J = 8.4 Hz, 1H), 8.05 (d, J = 8.0 Hz, 1H), 7.88 – 7.79 (m, 3H), 7.68 (t, J = 7.4 Hz, 3H), 7.62 (d, J = 8.5 Hz, 1H), 4.54 (s, 2H), 4.37 (s, 2H). ^{13}C NMR (101 MHz, DMSO) δ 164.08, 153.51, 147.01, 137.69, 135.55, 133.62, 130.76, 130.68, 128.88, 128.57, 127.69, 127.58, 127.46, 121.19, 50.67, 50.22. HRMS (AP-ESI) m/z Calcd for $C_{18}H_{17}N_3O_2$ $[M+H]^+$ 308.1394, found: 308.1389.

4.1.57 4-((((8-Chloroquinolin-2-yl)methyl)amino)methyl)-*N*-hydroxybenzamide (**14b**)

Using the synthetic method for **6a**, the target compound was obtained as a white solid in 33% yield. mp：147-150 °C. ^{1}H NMR (400 MHz, DMSO) δ 11.32 (s, 1H), 9.80 (s, 1H), 9.10 (s, 1H), 8.56 (d, J = 8.5 Hz, 1H), 8.04 (dd, J = 7.9, 3.2 Hz, 2H), 7.84 (d, J = 8.2 Hz, 2H), 7.78 (d, J = 8.5 Hz, 1H), 7.71 (d, J = 8.2 Hz, 2H), 7.66 (t, J = 7.9 Hz, 1H), 4.61 (s, 2H), 4.49 (s, 2H). ^{13}C NMR (101 MHz, DMSO) δ 164.07, 154.56, 142.93, 138.40, 135.58, 133.68, 132.32, 130.78, 130.73, 129.16, 128.07, 127.78, 127.61, 122.29, 50.63, 50.37. HRMS (AP-ESI) m/z Calcd for $C_{18}H_{16}ClN_3O_2$ $[M+H]^+$ 342.1004, found: 342.1006.

4.1.58 4-((((6-Bromoquinolin-2-yl)methyl)amino)methyl)-*N*-hydroxybenzamide (**14c**)

Using the synthetic method for **6a**, the target compound was obtained as a white solid in 36%

yield. mp：110-114°C. ^{1}H NMR (400 MHz, DMSO) δ 11.15 (s, 1H), 8.99 (s, 1H), 8.32 (d, J = 8.6 Hz, 1H), 8.26 (d, J = 1.8 Hz, 1H), 7.91 (d, J = 9.0 Hz, 1H), 7.86 (dd, J = 2.0 Hz, 1H), 7.72 (dd, J = 8.3, 4.6 Hz, 3H), 7.44 (d, J = 8.1 Hz, 2H), 3.96 (s, 2H), 3.79 (s, 2H). ^{13}C NMR (101 MHz, DMSO) δ 164.34, 162.41, 146.06, 144.02, 136.01, 132.90, 131.72, 131.12, 130.27, 128.75, 128.28, 127.20, 121.93, 119.22, 54.89, 52.60. HRMS (AP-ESI) m/z Calcd for $C_{18}H_{16}BrN_3O_2$ $[M+H]^+$ 386.0499, found: 386.0497.

4.1.59 *N*-hydroxy-4-((((6-methoxyquinolin-2-yl)methyl)amino)methyl)benzamide (**14d**)

Using the synthetic method for **6a**, the target compound was obtained as a white solid in 41% yield. mp：174-177 °C. ^{1}H NMR (400 MHz, DMSO) δ 11.35 (s, 1H), 9.94 (s, 1H), 9.10 (s, 1H), 8.33 (d, J = 8.5 Hz, 1H), 7.97 (d, J = 9.1 Hz, 1H), 7.82 (d, J = 8.1 Hz, 2H), 7.73 – 7.57 (m, 3H), 7.72 – 7.57 (m, 3H), 7.45 (dd, J = 9.4, 7.1 Hz, 2H), 4.44 (d, J = 8.0 Hz, 2H), 4.33 (s, 2H), 3.91 (s, 3H). ^{13}C NMR (101 MHz, DMSO) δ 164.08, 158.00, 150.65, 143.06, 136.45, 135.50, 133.60, 130.77, 130.35, 128.93, 127.57, 123.03, 121.57, 106.33, 56.07, 50.63, 50.14. HRMS (AP-ESI) m/z Calcd for $C_{19}H_{19}N_3O_3$ $[M+H]^+$ 338.1499, found: 338.1502.

4.1.60 4-((Benzyl(quinolin-2-ylmethyl)amino)methyl)-*N*-hydroxybenzamide (**16a**)

Using the synthetic method for **6a**, the target compound was obtained as a white solid in 45% yield. mp：90-92°C. ^{1}H NMR (400 MHz, DMSO) δ 11.15 (s, 1H), 8.95 (s, 1H), 8.36 (d, J = 8.5 Hz, 1H), 8.00 – 7.92 (m, 2H), 7.76 – 7.70 (m, 4H), 7.57 (t, J = 7.5 Hz, 1H), 7.51 (d, J = 8.1 Hz, 2H), 7.43 (d, J = 7.3 Hz, 2H), 7.35 (t, J = 7.5 Hz, 2H), 7.26 (t, J = 7.3 Hz, 1H), 3.81 (s, 2H), 3.64 (s, 2H), 3.60 (s, 2H). ^{13}C NMR (101 MHz, $CDCl_3$) δ 166.69, 160.48, 147.09, 143.52, 138.69, 136.84, 129.94, 129.68, 129.03, 128.84, 128.42, 128.37, 127.58, 127.38, 127.20, 127.03, 126.34, 120.87, 60.08, 58.49, 57.87. HRMS (AP-ESI) m/z Calcd for $C_{25}H_{23}N_3O_2$ $[M+H]^+$ 398.1863, found: 398.1856.

4.2. In vitro HDAC enzymatic assay

4.2.1. HeLa nuclear extracts

HDAC inhibitory activities of all the final products and the positive control drug Vorinostat were evaluated by the Color de Lys™ assay (BMLAK501, Enzo®Life Sciences) including HDAC1&2. Based on the HDAC kit instruction, HeLa cell nucleus extracts (HDAC1&2), substrate and tested compounds (including positive control compound) were diluted to needed concentrations. First, HeLa cell nucleus extracts (15μL/well) were incubated at 37°C for 5 min in the 96-well plate with different concentrations of tested compounds (10μL /well). Then substrate (25μL/well) was added and the mixture was incubating at 37°C for 30 min. At the end, the mixture of Color de Lys Developer and TSA (50μL/well) was added. After incubation for 30 min, the ultraviolet absorption was measured on a microtiterplate reader at 405 nm. The inhibition rates were calculated from the ultraviolet absorption of inhibited wells and control ones. A regression analysis method between the concentration and inhibition rate was used to give the IC_{50} values.

4.2.2. HDAC1, HDAC6 and HDAC8

All of the enzymatic reactions were conducted at 37°C for 30 minutes. The 50ul reaction mixture contains 25 mM Tris, pH 8.0, 1 mM $MgCl_2$, 0.1 mg/ml BSA, 137mM NaCl, 2.7 mM KCl, HDAC and the enzyme substrate. The compounds were diluted in 10% DMSO and 5μL of the

dilution was added to a 50μL reaction so that the final concentration of DMSO is 1% in all of reactions. The assay was performed by quantitating the fluorescent product amount of in solution following a enzyme reaction. Fluorescence is then analyzed with an excitation of 350-360 nm and an emission wavelength of 450-460 nm at SpectraMax M5 microtiter plate reader. The IC_{50} values were calculated using nonlinear regression with normalized dose-response fit in Prism GraphPad software.

4.3. MTT assay

All cell lines were cultured in RPMI1640 medium (10% FBS) at 37°C in a 5% CO_2 humidified incubator. Briefly, Cancer cells were plated at 4000–5000 cells per well (100 μL/well) in 96-well plates for 8 h and then treated with different concentrations of compounds (100 μL/well) for 48 h. 0.5% MTT solution (10 μL/well) was added and incubation for 4 h. DMSO (150 μL/well) was added to extract formazan formed from MTT. Absorbance was determined using a microtiter-plate reader at 570 nm. The IC_{50} values were calculated according to the inhibition ratios.

4.4. Whole-cell HDAC inhibition assay

The cellular HDAC assay was based on such assay described on patent WO20080952A1 with minor modifications. Briefly, human chronic myelogenous leukemia cell K562 were seeded into a 96-well tissue culture plates (Corning, Germany) at a density of 1.2×10^4 cells/well and incubation for 24 h. Then cells were treated with various concentrations of test compounds for 3 h. Substrates were added which Boc-Lys (acetyl)-AMC was used to measuring class I HDAC activity or Boc-Lys (triflouroacetyl)-AMC for measuring HDAC class IIa activity (final concentration: 0.2 mM). 3 h later under cell culture conditions, stop solution (50 mM Tris–HCl (pH 8.0), 137 mM NaCl, 2.7 mM KCl, 1 mM $MgCl_2$, 1% NP-40, 2.0 mg/mL trypsin, 10μM TSA) was added and the mixture was incubated for another 3 h. Fluorescence intensity was measured using a microplate reader at excitation and emission wavelengths of 360 and 470 nm, respectively.

4.5. Computational details

The crystal structure of HDAC1 (PDB: 5ICN [29]) was used in current study. PDB2PQR server was used to determine the protonation states of charged residues in HDAC1[30]. Specially, the protonation state of catalytic residues are determined based on our previous QM/MM study[31]. The initial structure of compound **4a** was built and minimized using Sybyl-X package. Molecular docking was performed using Autodock Vina[28] and the top-scored result was used as the starting conformation for MD simulation.

MD simulation was performed using Amber14 package[32] with Amber99SB[33] and TIP3P water model. Partial charges for compound **4a** was fit with HF/6-31G(d) calculations using Gaussian 09 package[34]. The HDAC1-**4a** system was neutralized with Cl^- counterions and solvated with explicit TIP3P water. Short-long effective function2 (SLEF2[35]) was introduced to describe charge interactions between the zinc ion and all other atoms. After a series of energy minimization and equilibration, 20ns standard molecular dynamics simulation was performed with periodic boundary condition. Other parameters were default values. All saved MD snapshots were analyzed using AmberTools 15. Figures are created using PyMOL (*The PyMOL Molecular Graphics System, Version 1.7. 4 Schrödinger, LLC.*).

Acknowledgments

This research was supported by the National Natural Science Foundation China (No. 81373281).

References

[1] E. Abdelfatah, Z. Kerner, N. Nanda, N. Ahuja, Epigenetic therapy in gastrointestinal cancer: the right combination, Therap. Adv. Gastroenterol., 9 (2016) 560-579.

[2] H. Zhang, Y.P. Shang, H.Y. Chen, J. Li, Histone deacetylases function as a novel potential therapeutic target for cancer, Hepatol. Res., (2016).

[3] Y. Zhang, H. Fang, J. Jiao, W. Xu, The structure and function of histone deacetylases: the target for anti-cancer therapy, Curr. Med. Chem., 15 (2008) 2840-2849.

[4] J. Roche, P. Bertrand, Inside HDACs with more selective HDAC inhibitors, Eur. J. Med. Chem., 121 (2016) 451-483.

[5] A. Vannini, C. Volpari, G. Filocamo, E.C. Casavola, M. Brunetti, D. Renzoni, P. Chakravarty, C. Paolini, R.D. Francesco, P. Gallinari, Crystal structure of a eukaryotic zinc-dependent histone deacetylase, human HDAC8, complexed with a hydroxamic acid inhibitor, Proceedings of the National Academy of Sciences, 101 (2004) 15064-15069.

[6] I. Oehme, H.E. Deubzer, D. Wegener, D. Pickert, J.P. Linke, B. Hero, A. Kopp-Schneider, F. Westermann, S.M. Ulrich, D.A. Von, Histone deacetylase 8 in neuroblastoma tumorigenesis, Clinical Cancer Research An Official Journal of the American Association for Cancer Research, 15 (2009) 91-99.

[7] H.M. Prince, M.J. Bishton, S.J. Harrison, Clinical studies of histone deacetylase inhibitors, Clin. Cancer Res., 15 (2009) 3958-3969.

[8] P.S. Suresh, V.C. Devaraj, N.R. Srinivas, R. Mullangi, Review of bioanalytical assays for the quantitation of various HDAC inhibitors such as vorinostat, belonistat, panobinostat, romidepsin and chidamine, Biomed. Chromatogr., (2016).

[9] B.S. Mann, J.R. Johnson, M.H. Cohen, R. Justice, R. Pazdur, FDA approval summary: vorinostat for treatment of advanced primary cutaneous T-cell lymphoma, Oncologist, 12 (2007) 1247-1252.

[10] R. Frye, M. Myers, K.C. Axelrod, E.A. Ness, R.L. Piekarz, S.E. Bates, S. Booher, Romidepsin: a new drug for the treatment of cutaneous T-cell lymphoma, Clin. J. Oncol. Nurs., 16 (2012) 195-204.

[11] H.Z. Lee, V.E. Kwitkowski, P.L. Del Valle, M.S. Ricci, H. Saber, B.A. Habtemariam, J. Bullock, E. Bloomquist, Y. Li Shen, X.H. Chen, J. Brown, N. Mehrotra, S. Dorff, R. Charlab, R.C. Kane, E. Kaminskas, R. Justice, A.T. Farrell, R. Pazdur, FDA Approval: Belinostat for the Treatment of Patients with Relapsed or Refractory Peripheral T-cell Lymphoma, Clin. Cancer Res., 21 (2015) 2666-2670.

[12] J.P. Laubach, P. Moreau, J.F. San-Miguel, P.G. Richardson, Panobinostat for the Treatment of Multiple Myeloma, Clin. Cancer Res., 21 (2015) 4767-4773.

[13] S. Yoon, G.H. Eom, HDAC and HDAC Inhibitor: From Cancer to Cardiovascular Diseases, Chonnam Med. J., 52 (2016) 1-11.

[14] P. Guan, F. Sun, X. Hou, F. Wang, F. Yi, W. Xu, H. Fang, Design, synthesis and preliminary bioactivity studies of 1,3,4-thiadiazole hydroxamic acid derivatives as novel histone deacetylase inhibitors, Bioorg. Med. Chem., 20 (2012) 3865-3872.

[15] P. Guan, L. Wang, X. Hou, Y. Wan, W. Xu, W. Tang, H. Fang, Improved antiproliferative activity of 1,3,4-thiadiazole-containing histone deacetylase (HDAC) inhibitors by introduction of the heteroaromatic surface recognition motif, Bioorg. Med. Chem., 22 (2014) 5766-5775.

[16] H. Fu, L. Han, X. Hou, Y. Dun, L. Wang, X. Gong, H. Fang, Design, synthesis and biological evaluation of saccharin-based N-hydroxybenzamides as histone deacetylases (HDACs) inhibitors, Bioorg. Med. Chem., 23

(2015) 5774-5781.

[17] R. Liu, J. Wang, W. Tang, H. Fang, Design and synthesis of a new generation of substituted purine hydroxamate analogs as histone deacetylase inhibitors, Bioorg. Med. Chem., 24 (2016) 1446-1454.

[18] J. Wang, F.e. Sun, L. Han, X. Hou, X. Pan, R. Liu, W. Tang, H. Fang, Design, synthesis, and preliminary bioactivity studies of substituted purine hydroxamic acid derivatives as novel histone deacetylase (HDAC) inhibitors, MedChemComm, 5 (2014) 1887-1891.

[19] F.W. Peng, J. Xuan, T.T. Wu, J.Y. Xue, Z.W. Ren, D.K. Liu, X.Q. Wang, X.H. Chen, J.W. Zhang, Y.G. Xu, L. Shi, Design, synthesis and biological evaluation of N-phenylquinazolin-4-amine hybrids as dual inhibitors of VEGFR-2 and HDAC, Eur. J. Med. Chem., 109 (2016) 1-12.

[20] L. Wang, X. Hou, H. Fu, X. Pan, W. Xu, W. Tang, H. Fang, Design, synthesis and preliminary bioactivity evaluations of substituted quinoline hydroxamic acid derivatives as novel histone deacetylase (HDAC) inhibitors, Bioorg. Med. Chem., 23 (2015) 4364-4374.

[21] R. Cincinelli, V. Zwick, L. Musso, V. Zuco, M. De Cesare, F. Zunino, C. Simoes-Pires, A. Nurisso, G. Giannini, M. Cuendet, S. Dallavalle, Biphenyl-4-yl-acrylohydroxamic acids: Identification of a novel indolyl-substituted HDAC inhibitor with antitumor activity, Eur. J. Med. Chem., 112 (2016) 99-105.

[22] F. Thaler, L. Moretti, R. Amici, A. Abate, A. Colombo, G. Carenzi, M.C. Fulco, R. Boggio, G. Dondio, S. Gagliardi, S. Minucci, L. Sartori, M. Varasi, C. Mercurio, Synthesis, biological characterization and molecular modeling insights of spirochromanes as potent HDAC inhibitors, Eur. J. Med. Chem., 108 (2016) 53-67.

[23] C. De Souza, B.P. Chatterji, HDAC Inhibitors as Novel Anti-Cancer Therapeutics, Recent Pat. Anticancer Drug Discov., 10 (2015) 145-162.

[24] T. Tashima, H. Murata, H. Kodama, Design and synthesis of novel and highly-active pan-histone deacetylase (pan-HDAC) inhibitors, Bioorg. Med. Chem., 22 (2014) 3720-3731.

[25] Z. Deng, X. Liu, J. Jin, H. Xu, Q. Gao, Y. Wang, J. Zhao, Histone Deacetylase Inhibitor Trichostatin a Promotes the Apoptosis of Osteosarcoma Cells through p53 Signaling Pathway Activation, Int. J. Biol. Sci., 12 (2016) 1298-1308.

[26] Y. Li, K. Zhao, C. Yao, S. Kahwash, Y. Tang, G. Zhang, K. Patterson, Q.E. Wang, W. Zhao, Givinostat, a type II histone deacetylase inhibitor, induces potent caspase-dependent apoptosis in human lymphoblastic leukemia, Genes Cancer, 7 (2016) 292-300.

[27] R.D. Kelly, S.M. Cowley, The physiological roles of histone deacetylase (HDAC) 1 and 2: complex co-stars with multiple leading parts, Biochem. Soc. Trans., 41 (2013) 741-749.

[28] O. Trott, A.J. Olson, AutoDock Vina: improving the speed and accuracy of docking with a new scoring function, efficient optimization, and multithreading, J. Comput. Chem., 31 (2010) 455-461.

[29] P.J. Watson, C.J. Millard, A.M. Riley, N.S. Robertson, L.C. Wright, H.Y. Godage, S.M. Cowley, A.G. Jamieson, B.V.L. Potter, J.W.R. Schwabe, Insights into the activation mechanism of class I HDAC complexes by inositol phosphates, Nature Communications, 7 (2016) 11262.

[30] S. Unni, Y. Huang, R.M. Hanson, M. Tobias, S. Krishnan, W.W. Li, J.E. Nielsen, N.A. Baker, Web servers and services for electrostatics calculations with APBS and PDB2PQR, J. Comput. Chem., 32 (2011) 1488-1491.

[31] R. Wu, S. Wang, N. Zhou, Z. Cao, Y. Zhang, A Proton-Shuttle Reaction Mechanism for Histone Deacetylase 8 and the Catalytic Role of Metal Ions, J. Am. Chem. Soc., 132 (2010) 9471-9479.

[32] Case, D.A., Babin, V., Berryman, J., Betz, R.M., Cai, Q., Cerutti, D.S., Cheatham Iii, T.E., Darden, T.A., Duke, R.E., Gohlke, H. and Goetz, A.W., 2014. Amber 14.

[33] (a) Cornell, W. D.; Cieplak, P.; Bayly, C. I.; Gould, I. R.; Merz, K. M.; Ferguson, D. M.; Spellmeyer, D. C.;

Fox, T.; Caldwell, J. W.; Kollman, P. A. J. Am. Chem. Soc. 1995, 117, 5179–5197.

(b) Wang, J. M.; Cieplak, P.; Kollman, P. A. J. Comput. Chem. 2000, 21, 1049–1074.

(c) Hornak, V.; Abel, R.; Okur, A.; Strockbine, B.; Roitberg, A.; Simmerling, C. Proteins: Struct., Funct., Bioinf. 2006, 65, 712–725

[34] Frisch, M.J., Trucks, G.W., Schlegel, H.B., Scuseria, G.E., Robb, M.A., Cheeseman, J.R., Scalmani, G., Barone, V., Mennucci, B. and Petersson, G.A., 2009. Gaussian software, version 09 revision D01. Gaussian Inc.: Wallingford, CT, USA.

[35] W. Gong, R. Wu, Y. Zhang, Thiol versus hydroxamate as zinc binding group in HDAC inhibition: An Ab initio QM/MM molecular dynamics study, J. Comput. Chem., 36 (2015) 2228-2235.

1. Novel quinoline-based N-hydroxycinnamamides were designed and synthesized.

2. Compound **4a** showed better inhibitory activity for class I HDAC than Vorinostat.

3. Compound **4e** exhibited excellent anti-proliferative activity against K562.

4. Compound **4a** and **4e** could promote cell apoptosis in vitro.